

ADVANCES IN ULTRAFAST RADIATIVE TRANSFER MODELING AND APPLICATIONS: A REVIEW

Zhixiong Guo* & Brian Hunter

Department of Mechanical and Aerospace Engineering, Rutgers, The State University of New Jersey, 98 Brett Road, Piscataway, NJ 08854

*Address all correspondence to Zhixiong Guo E-mail: guo@jove.rutgers.edu

The use of ultrafast laser technology has become widespread in recent years for many emerging applications, such as optical tomography, plasma-mediated ablation, surgical and medical procedures, and device manufacturing and material microprocessing for both biomedical and industrial purposes. In situations where ultrafast laser experimentation is complicated or expensive, numerical modeling can be implemented as a realistic alternative. In optical imaging reconstruction, forward modeling of radiative transfer under various conditions is indispensable. To determine radiant energy propagation with ultrafast speed of light, an accurate solution of the time-dependent hyperbolic equation of radiative transfer is required; and this is featured as ultrafast radiative transfer. In this review, advances in the computational modeling of ultrafast radiative transfer are discussed. Various numerical solution methodologies, along with the mentioning of their contributing works, advantages and challenges, are presented. The importance of appropriate treatment of anisotropic scattering of both ballistic and diffuse radiations is addressed. Additionally, specific applications of ultrafast laser technology in the biomedical field are presented, along with contributing works.

KEY WORDS: radiation transfer, anisotropic scattering, normalization of phase function, discrete-ordinates method, finite-volume method, Monte Carlo method, diffusion approximation, ultrafast phenomena

1. INTRODUCTION

In the past two decades, the use of ultrashort-pulsed (USP) lasers for both fundamental scientific research and biomedical and industrial applications has increased greatly, due to the increasing affordability of equipment, a more sophisticated understanding of the advantages of the aforementioned technology, and exploration of emerging ultrafast phenomena. When a powerful USP laser beam is converged to a small spot, the energy flux at the focus can be over a threshold that induces optical breakdown, opening up a brand new window of nonlinear optics. One example of applications is plasma-mediated ablation and micromachining of basically any material including transparent or low-absorption materials (Niemz et al., 1991; Liu et al., 1997; Loesel et al., 1998; Choi and Grigoropoulos, 2002; Hong et al.,

NOMENCLATURE

c	speed of light in a medium	σ_a	absorption coefficient, m^{-1}
g	asymmetry factor	σ_s	scattering coefficient, m^{-1}
G	incident radiation, W/m^2	μ, η, ξ	direction cosines
I	radiative intensity, $\text{W}/\text{m}^2 \cdot \text{sr}$	Φ	scattering phase-function
I^B	ballistic irradiance, W/m^2	ω	scattering albedo, $= \sigma_s/(\sigma_a + \sigma_s)$
\mathbf{r}	position vector		
$\hat{\mathbf{s}}$	unit direction vector		
t	time		
w	directional weight		
	Greek symbols		
β	extinction coefficient, m^{-1}		
			Superscripts
		B	ballistic component
		'	radiation incident direction
		l, l'	radiation directions
		$l'l$	from direction l' to l

2004; Chowdhury et al., 2005; Huang and Guo, 2009b, 2010; Wang and Guo, 2010). Due to the ultrafast pulse duration being much shorter than the thermal relaxation time of materials, thermal diffusion hardly occurs during the process, resulting in elimination/minimization of thermal and mechanical damage (Huang and Guo, 2009b, 2010; Wang and Guo, 2010) that is usually a concern with the application of conventional continuous-wave (CW) or pulsed lasers. When a relatively weak USP laser is used for diagnostics, the information contained in a broadened transient signature is more abundant (Yamada, 1995; Kumar and Mitra, 1999; Guo et al., 2002).

Ultrafast laser technology has exerted an especially significant impact on the field of biomedicine. The advent of USP laser technology allowed for great advances in the near-infrared optical imaging (Wang et al., 1991; Liu et al., 1993; Yoo and Alfano, 1993; Gu and Sheppard, 1995; Hielscher et al., 1995b; Yodh and Chance, 1995; Alfano et al., 1997; Villringer and Chance, 1997; Quan and Guo, 2004) of growths embedded in biological tissue, such as cancerous tumors. In addition, ultrafast lasers have become widely used for other biomedical therapeutic applications, such as precision laser microsurgery (Wang et al., 1991), tissue ablation and microprocessing (Kim et al., 2001; Huang and Guo, 2009a), decontamination of transplants or medical devices (Guo et al., 2010; Wang and Guo, 2010), and laser tissue welding (Fried et al., 1999; Kim and Guo, 2004). USP lasers have a distinct advantage over CW or general pulsed lasers in regard to heating/removal of cancerous tumors, as the pulse duration is much shorter than the thermal relaxation time (Kim and Guo, 2007; Jiao and Guo, 2009). This allows the laser beam to interact with the tumor before heat diffusion ever occurs, resulting in a minimization of thermal damage to the surrounding healthy tissue while increasing

the tumor temperature greatly in a short period of time or completely removing the target cancerous tissue.

Advances in the ultrafast laser technology and applications have also spurred increases in numerical research. In the cases where experimental research is expensive or potentially dangerous, numerical modeling is an appreciable alternative. In reconstruction of optical images, intensive modeling is indispensable. Radiation is the dominant mode of energy transfer in ultrafast laser applications, and thus the overall impact of ultrafast laser irradiation can be determined through accurate solution of the Equation of Radiative Transfer (ERT). Traditional explorations of numerical radiative heat transfer neglected the effects of speed-of-light propagation, even in the cases involving time-dependent boundary conditions (the so-called traditional transient radiative transfer). Such exclusion does not result in any practical errors for most traditional radiation engineering problems (Modest, 2002; Howell et al., 2010), because the imposed temporal variations are much slower when compared with the time scale associated with the speed of radiation wave propagation in the system. However, when the ultrafast time scale due to USP irradiation is concerned, neglect of wave propagation in the ERT will have a drastic impact on radiative transfer predictions (Mitra et al., 1997; Kumar and Mitra, 1999; Wu and Wu, 2000; Guo and Kumar 2001a,b, 2002). It is essential that the ultrafast time dependence in the governing hyperbolic wave equation be incorporated in the case where the wave-propagation time in a system is not much shorter than the characteristic time of event variation (such as pulse width) (Guo and Kumar, 2001b). Other examples in which wave propagation is critical include radiation in the outer-space astrophysics. In order to differentiate the wave-propagation radiation transfer from the traditional transient radiation transfer where the ERT itself is still stationary, Kim and Guo (2004) first introduced the terminology of ultrafast radiative transfer in 2004. This new terminology captures exactly the ultrafast feature and phenomenon of radiation wave propagation, rather than a simple time dependence as in traditional transient problems; and thus, should be adopted in the field. The general vector form of the ultrafast wave propagation transient ERT (TERT) is given, as follows:

$$\begin{aligned} \frac{1}{c} \frac{\partial I(\mathbf{r}, \hat{s}, t)}{\partial t} + \hat{s} \cdot \nabla I(\mathbf{r}, \hat{s}, t) = & -(\sigma_a + \sigma_s) I(\mathbf{r}, \hat{s}, t) \\ & + \sigma_a I_b(\mathbf{r}, t) + \frac{\sigma_s}{4\pi} \int_{4\pi} I(\mathbf{r}, \hat{s}', t) \Phi(\hat{s}', \hat{s}) d\Omega'. \end{aligned} \quad (1)$$

In the preceding equation, $I(\mathbf{r}, \hat{s}, t)$ represents the radiant intensity at a given location \mathbf{r} and time t propagating in the radiation direction \hat{s} , σ_a and σ_s are the medium absorption and scattering coefficients, and c is the speed of light in the medium. The first temporal term on the left-hand side of the equation is an addition to steady-state ERT, representing the propagation of radiant energy with a wave at the speed of light. Thus, the TERT is not only an integro-differential

equation but also a hyperbolic wave equation. Analytical solution is nearly impossible, save for a few simplistic cases.

Various numerical methods have been developed as a means of solving the TERT for accurately determining radiation propagation. In this review, advances in the numerical modeling of ultrafast radiative transfer are discussed in detail. The major numerical TERT solution methods, along with the mentioning of their contributing works, advantages, and disadvantages, are discussed. In addition, some computational results are presented in order to fully clarify the capabilities of numerical modeling of ultrafast radiative transfer. Since light scattering in biological tissues is generally highly anisotropic and the propagation of a laser beam consists of both ballistic and diffuse components, recent development of the normalization of ballistic and diffuse scattering phase functions is emphasized. Finally, specific applications of ultrafast laser technology in the field of biomedicine, along with notable contributing works, are reviewed.

2. DIFFUSION APPROXIMATION

The Diffusion Approximation (DA), first introduced by Rosseland (1936) as a means of determining photon transport in stellar bodies, is a widely-used technique for describing photon migration and particle transport in diffuse media. In general, the integro-differential ERT is extremely difficult to solve analytically when scattering is dominant. Using the DA, the integral dependence of the governing equation is eliminated, and the ERT is approximated using partial-differential equations, which can be solved more easily. The DA is a simplified formula for the ERT for diffuse media; however, there are many inherent limitations on the usefulness of this approximation.

To determine the governing equation for the DA in ultrafast radiative transfer, the TERT is first expanded using spherical harmonics (Menguc and Viskanta, 1983), resulting in a set of coupled partial differential equations, known as the P_N approximation. Retaining the first term of the TERT (known as the P_1 expansion), we obtain the governing equation for the DA, or the diffusion equation, as follows (Furutsu, 1980; Ishimaru, 1989):

$$\frac{1}{c} \frac{\partial \phi(\mathbf{r}, t)}{\partial t} + \nabla \cdot (D \nabla \phi(\mathbf{r}, t)) + \sigma_a \phi(\mathbf{r}, t) = Q(\mathbf{r}, t). \quad (2)$$

In the governing equation, $\phi(\mathbf{r}, t) = \frac{1}{4\pi} \int_{4\pi} I(\mathbf{r}, \hat{\mathbf{s}}, t) d\Omega$ is the photon fluence rate,

$Q(\mathbf{r}, t)$ is the source term from the input distribution, and D is the diffusion coefficient. A complete derivation of the diffusion equation from the space-time transport equation is presented by Furutsu (1980). This equation is known as the "diffusion equation" due to its similarity to the heat diffusion equation, and solutions can be easily obtained using numerical techniques or commercial software

(Guo et al., 2003). This equation can also be solved analytically in some simple cases.

There has been considerable debate about the expression of the diffusion coefficient D . The traditional expression for the diffusion coefficient is given as follows (Ishimaru, 1989; Patterson et al., 1989; Guo et al., 2003):

$$D_1 = \frac{1}{3[(1-g)\sigma_s + \sigma_a]} = \frac{1}{3[\sigma'_s + \sigma_a]}, \quad (3)$$

where σ'_s is the reduced scattering coefficient. However, a theoretical investigation into the diffusion coefficient by Furutsu and Yamada (1994) claimed that the diffusion coefficient should be independent of the absorption coefficient, or

$$D_2 = \frac{1}{3\sigma'_s}. \quad (4)$$

This claim was further supported by Durduran et al. (1997), who found that using Eq. (4) to describe the diffusion coefficient produced more accurate results when compared with the Monte Carlo simulation, and Bassani et al. (1997), who verified the use of Eq. (4) by both Monte Carlo simulation and performing experiments on a suspension of calibrated polystyrene spheres irradiated with a He-Ne laser. In addition, a study by Cai et al. (2002) indicated that the diffusion coefficient has temporal dependence. They noted that, while the diffusion coefficient approximates Eq. (4) after long periods of time, the diffusion coefficient is noticeably smaller at short times. However, they also acknowledged that this change in the diffusion coefficient cannot be accounted for by Eq. (3), due to their finding that the diffusion coefficient was indeed independent of the absorption coefficient.

Ishimaru (1989) investigated the diffusion of light in turbid media, such as a biological tissue, using the DA. While he concluded that, at the time of publication, the DA was the most accurate approximate method for predicting light diffusion, he also noted some major limitations. Via comparison of DA predictions with experimental data, he noted that the DA was an excellent approximation only for the case where the optical thickness was much greater than unity, the asymmetry factor much smaller than unity, and the scattering albedo was close to unity. In addition, it was noted that the DA is an approximation representing the limiting case where multiple scattering dominates, and that it may not be applicable near a boundary surface where first-order scattering dominates. A major finding of Ishimaru's work was that the DA predicts the propagation speed of a diffuse pulse as $c/(n\sqrt{3})$, instead of the theoretical value c/n , where n is the refractive index of the medium.

Yoo et al. (1990) further investigated the conditions for which the DA would fail in predicting photon transport in random media. They experimentally measured the temporal distribution of photons, generated by a 100 fs mode-locked laser, that were scattered out of a pin hole after being passed through a random medium of

water and latex beads and compared the results with DA predictions. They found that the transport of photons through this random media deviated from the DA when the medium thickness was much smaller than the transport mean free path. In addition, they found that photons are found to arrive earlier than predicted by the diffusion theory as the optical thickness becomes smaller than the mean free path and as the degree of medium anisotropy increases.

Although there are many inherent limitations for the DA, as discussed, it has been widely used and compared with experimental data for determining photon migration in biological tissues, due to the simplicity of numerical implementation. Patterson et al. (1989) used the DA as a means of measuring the optical properties of tissue by examining the time-resolved reflectance and transmittance. They noted that the temporal characteristics of both transmitted and reflected light carry information about the absorption and scattering coefficients of tissue. Brewster and Yamada (1995) also investigated the determination of optical properties in turbid media from temporal light scattering measurements. They investigated light propagation in an optically thick, plane parallel homogeneous slab of turbid media subjected to a collimated pulsed incident radiation. Comparisons between the DA, Monte Carlo, and experiment were made to assess the validity of using the DA to determine optical properties. While it was found that the Monte Carlo results were more accurate when compared to experiment, they claimed that the diffusion theory predictions of log slope and pulse width were accurate enough to determine optical properties from time-resolved transmittance and reflectance measurements.

Arridge et al. (1992) further implemented the DA in order to determine optical pathlengths in tissues. They investigated measurements in both the time and frequency domains for a variety of geometries commonly seen in clinical applications, relating the mean optical pathlength in tissue to the phase delay of an intensity-modulated optical carrier. They also showed that, for the human brain tissue, mean time and phase correlate very closely, indicating that phase measurements could be used as an alternate means of monitoring optical pathlength in the brain. A further work by Firbank et al. (1996) investigated the impact of clear cerebrospinal fluid on light distribution in the brain, comparing the DA and Monte Carlo light propagation predictions to the solid slab phantom experiments. It was seen that the DA was not able to accurately model the impact of the clear layer on light distribution witnessed in both experimental and Monte Carlo results.

Yamada and Hasegawa (1996) solved the DA equation using the finite element method, comparing temporal transmittance variations through both scattering slabs and cylinders to Monte Carlo results. They found that the Monte Carlo method results were more accurate than the DA predictions, in general, but came at the cost of computational efficiency. There have been many other investigations into photon migration and time-resolved measurements using the DA. Hielscher et al. (1995a) investigated the application of the diffusion theory for optical property determination from time-resolved reflectance, specifically comparing the DA with

Monte Carlo predictions for three different types of boundary conditions. Kienle et al. (1998) investigated the propagation of light in a two-layered turbid media with an infinitely thick second layer using time-resolved reflectance, using the DA to show the ability of deriving the absorption and reduced scattering coefficients of the entire medium if the first layers' thickness and time-resolved reflectance are known. Contini et al. (1997) analyzed the time-dependent diffusion equation with solutions for both slab and semi-infinite diffusing media subjected to either a time-dependent or continuous wave source.

Aiming at improving the solutions of the diffusion equation, Kienle and Patterson (1997) performed a study to show that solutions of the diffusion equation that use extrapolated boundary conditions, which had been previously shown to contain large errors when examining reflectance from a semi-infinite medium, could be improved using a frequency domain technique by which the time-resolved reflectance was calculated using integration of reflected radiance instead of the gradient of fluence rate. They found that errors in deriving optical coefficients were considerably smaller for this improvement than commonly used solutions, which was verified by experiment. Gershenson (1999) further used a higher-order spherical-harmonic expansion of the TERT, finding that this improvement predicted the intensity for multiple scattering at earlier times and shorter distances than the traditional diffusion equation. Further, it was discussed that while second-order corrections to the diffusion equation appear in literature, they may not be valid.

In a later work, Guo et al. (2003) compared the use of the DA with both the Monte Carlo Method (MCM) and Transient Discrete-Ordinates Method (TDOM) for describing light transport in tissues. In their work, they investigated the ultrafast transport of light through 2D rectangular or 3D cubic enclosures containing a relatively low-scattering inhomogeneity of different sizes, locations, and nature. The enclosure was irradiated at one wall by a laser source with Gaussian profile. While they noted that the DA was more computationally efficient than the DOM, they found that the differences between the DA and the DOM and MCM predictions were obvious even for optically very thick media. The DA completely failed in predicting the ballistic transport of photons, and was not able to predict the photon "snake" effect. An increase in the size of the low-scattering inhomogeneous layer in the medium produced larger differences between DA and MCM solutions. This fact can be seen in Fig. 1, as normalized intensity profiles predicted by the DA differ greatly from those predicted using the DOM radiative transfer (RT) modeling and the MCM simulation at specific detector locations in the medium. The difference of the DA results between the two different diffusion coefficients is slight.

An overview of the use of the diffusion approximation for the study of photon migration in a biological tissue for such applications as optical tomography was presented by Yamada (2000). In recent years, the advent of high-speed/power computing workstations has reduced the necessary computational time for the more

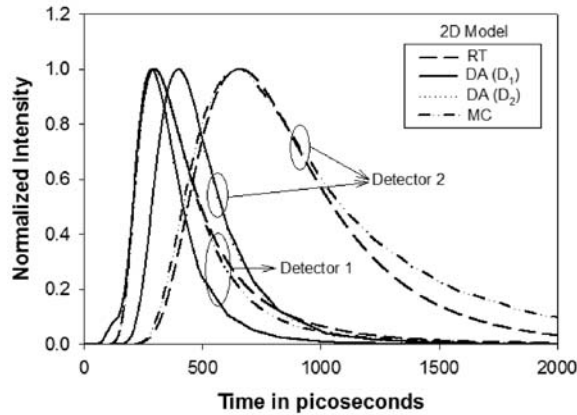


FIG. 1: Comparison of temporal normalized intensity at two detector locations among the DA with two different diffusion coefficients and the DOM radiative transfer (RT) computation and the MCM simulation in a multilayer brain tissue model [reproduced from (Guo et al., 2003)]

accurate approximate methods like DOM and Finite Volume Method (FVM), thus making the inherent computational efficiency of the DA less crucial. Although this method does have built-in flaws and limitations, it remains the simplest method for determining photon migration in many cases with varying optical properties.

3. DISCRETE-ORDINATES METHOD

3.1 Governing Equations

One commonly used approximate method for solving the steady-state ERT, due to the relative simplicity of numerical implementation and computational efficiency, is the S_N Discrete-Ordinates Method (DOM) (Fiveland, 1984), which was first introduced by Chandrasekhar (1960) for atmospheric and astrophysical radiation and by Carlson and Lathrop (1968) as a means of solving the neutron-transport equation. For this method, the continuous directional variation of radiative intensity in the ERT is represented by a finite number of discrete directions (or ordinates) spanning the full 4π solid angle range (Modest, 2002). Use of discrete directions allows all solid-angle integrations to be approximated by numerical quadrature sums, thus fully converting the integro-differential ERT into a set of partial differential equations. Removal of the integral dependency of the governing equation greatly simplifies the ERT solution process.

For the general three-dimensional enclosure that can be described by Cartesian coordinates, Eq. (1) can be expressed using the transient DOM (TDOM) as follows (Guo and Kumar, 2002):

$$\frac{1}{c} \frac{\partial I^l}{\partial t} + \mu^l \frac{\partial I^l}{\partial x} + \eta^l \frac{\partial I^l}{\partial y} + \xi^l \frac{\partial I^l}{\partial z} = -(\sigma_a + \sigma_{sm})I^l + S^l, l = 1, 2, \dots, M. \quad (5)$$

In the preceding equation, I^l is the radiant intensity propagating in a discrete direction \hat{s}^l ; ξ^l , η^l , and μ^l are the direction cosines in the x , y , and z directions, respectively; σ_{sm} is the modified scattering coefficient (Chai et al., 1998), and M is the total number of discrete directions.

The radiative source term S^l and modified scattering coefficient σ_{sm} can be expressed in the following manner:

$$S^l = \sigma_a I_b + \frac{\sigma_s}{4\pi} \left(\sum_{\substack{i=1 \\ i \neq l}}^M w^i \Phi^{i'l} I^i + \sum_B I^B \Phi^{l^B} \right), \tag{6a}$$

$$\sigma_{sm} = \sigma_s \left(1 - \frac{1}{4\pi} w^l \Phi^{ll} \right), \tag{6b}$$

where the in-scattering integral in the original governing equation has been replaced by a summation over all discrete directions. Here, I_b is the blackbody emissive intensity of the medium, $\Phi^{i'l}$ is the scattering phase function representing the scattering of radiant energy between two discrete directions, and w^i is the discrete direction weighting factor corresponding to \hat{s}^i . In order to increase DOM computational efficiency for strongly scattering media, a modified scattering coefficient can be introduced following the treatment of Chai et al. (1998), in which the forward-scattering term is removed from the summation and treated as transmission.

The third term in Eq. (6a) represents the in-scattering of ballistic radiation, which becomes important in applications involving irradiation by collimated solar or laser incidence, or a focused ballistic laser beam cone. In the aforementioned term, I^B is the ballistic irradiance (incident heat flux) at a given medium location, and Φ^{l^B} is the ballistic scattering phase function between the direction of ballistic incidence \hat{s}^B and discrete direction \hat{s}^l . As an example, for a medium being irradiated by a normally incident collimated laser acting in the x direction, the ballistic intensity I^B at any location in the medium can be represented as follows (Guo and Kim, 2003)

$$I^B(x, y, z, \xi^B, t) = I_o \left(x = 0, y, z, t - \frac{x}{c\xi^B} \right) \exp\left(-\frac{\beta x}{\xi^B}\right) \delta(\xi^B - 1), \tag{7}$$

where I_o is the irradiated laser power flux at the tissue surface (excl. reflection), $\beta = \sigma_a + \sigma_s$ is the overall extinction coefficient, and δ is the Dirac delta function.

For radiative transfer analysis of a medium being irradiated by a USP laser, the medium can be treated as cold because the blackbody emission intensity is always much smaller than the incident laser intensity, and thus is negligible. For cases where a medium is irradiated by a continuous pulse train, Duhamel's superposition

theorem can be used to construct the response of a medium to pulse train irradiation from the response of a single pulse. This method was first constructed by Guo and Kumar (2002), and expanded on by Liu and Hsu (2008), as well as Akamatsu and Guo (2011).

Although the choice of a quadrature scheme for the DOM is arbitrary, the chosen discrete directions and weighting factors must satisfy certain conditions. Commonly, the S_N quadrature is implemented, and the highest quadrature available in the literature is the S_{16} quadrature (288 total discrete directions). Quadrature sets for S_8 to S_{12} are available from Fiveland (1991), while S_{14} and S_{16} are available from the TWOTRAN code of Lathrop and Brinkley (1973).

Once the intensity field in the medium is obtained through solution of Eq. (5), the incident radiation G and the net radiative heat flux in the x direction at any location in the medium can be calculated using the following summations:

$$G = \sum_{l=1}^M I^l w^l + \sum_B I^B, \quad (8a)$$

$$Q_x = \sum_{l=1}^M \mu^l I^l w^l + \sum_b \mu^b I^b. \quad (8b)$$

Expressions for the net radiative heat flux in the y and z directions can be determined by simple manipulation of the direction cosine in Eq. (8b). Finally, the transient divergence of radiative heat flux can be calculated using the expression

$$\nabla \cdot q_r = \beta (1 - \omega) (4\pi I_b - G) - \frac{1}{c} \frac{\partial G}{\partial t}, \quad (9)$$

where the transient term, communicated by Rath and Mahapatra (2012) as discussed in Hunter and Guo (2012b), is not related directly to medium energy deposition. Rather, this transient term describes the propagation of radiant energy with a wave through the medium, accounting for the amount of energy that is physically "trapped" in a given control volume at a specific time instant that will travel to adjacent control volumes at subsequent times without being physically absorbed by the medium (Hunter and Guo, 2012b).

3.2 Numerical Scheme

In order to solve the series equations in (5), the general three-dimensional enclosure is subdivided into a number of small control volumes. The temporal and spatial derivatives in the governing equations are approximated using control-volume techniques. After both spatial and temporal discretization, Eq. (5) can be expressed, for a discrete direction \hat{s}^l , for a given spatial control volume as follows (Guo and Kumar, 2002):

$$\begin{aligned}
& \frac{1}{c\Delta t} \left(I_p^l - I_p^{l0} \right) + \frac{|\xi^l|}{\Delta x} \left(A_{xu}^l I_{xu}^l - A_{xd}^l I_{xd}^l \right) + \frac{|\eta^l|}{\Delta y} \left(A_{yu}^l I_{yu}^l - A_{yd}^l I_{yd}^l \right) + \frac{|\mu^l|}{\Delta z} \left(A_{zu}^l I_{zu}^l - A_{zd}^l I_{zd}^l \right) \\
& = - \left(\sigma_{a,p} + \sigma_{sm,p} \right) I_p^l + S_p^l .
\end{aligned} \tag{10}$$

In the preceding equation, the subscript p indicates the central node of a given control volume; I_p^{l0} is the radiant intensity at node p and in direction \hat{s}^l at the previous time step; A_{xu}^l , A_{yu}^l , and A_{zu}^l are the facial areas of the upstream control-volume surfaces; A_{xd}^l , A_{yd}^l , and A_{zd}^l are the facial areas of the downstream control-volume surfaces; I_{xu}^l , I_{yu}^l , and I_{zu}^l are the radiant intensities located at the upstream faces of the control-volume in direction l , and I_{xd}^l , I_{yd}^l , and I_{zd}^l are the radiant intensities located at the downstream faces of the control volume. The details for solving Eq. (10) have been described in (Guo and Kumar, 2002), and thus are not repeated here.

The use of both temporal and spatial differencing to approximate derivatives makes the TDOM susceptible to false scattering (numerical diffusion) (Chai et al., 1993), which is one of the main drawbacks of using the DOM. As described by Modest (2002), if a single collimated ray of radiant energy is traced through an enclosure using this method, the beam will unrealistically widen and smear as it moves farther from the origin point, even when real scattering does not exist. False scattering can be mitigated by ensuring that the spatial and temporal grid sizes are as small as possible. Further, the time step Δt must satisfy the following condition (Guo and Kumar, 2001a):

$$c\Delta t \leq \min(\Delta x, \Delta y, \Delta z) , \tag{11}$$

so that the traveling distance of a ray of light between two consecutive time steps does not exceed the size of the control volume. While the grid sizes can be further refined in order to limit the error stemming from false scattering, an increase in the number of control volumes leads to dramatic increases in computational convergence time for the intensity field.

A second major drawback of the DOM, and any other schemes that approximate the continuous angular variation with a finite number of directions, is the appearance of ray effect (Chai et al., 1993). As radiant energy travels away from a source in discrete directions, it is possible that far from the emission point the rays will become so spread out that certain surfaces or control volumes will not receive any energy contribution. This lack of energy propagation to certain locations due to the finite number of radiation directions at the source can cause physically unrealistic bumps in the heat flux profiles. The ray effect is much more pronounced for optically thin media than optically thick ones, and can be decreased via an increase in the number of discrete directions (Chai et al., 1993). The ray effect was also found not to occur consistently between the DOM and

FVM in transient and steady-state radiative transfer (Hunter and Guo, 2011), due to the inherent difference in the chosen discrete directions. Recently, Huang et al. (2011) claimed a method to mitigate the appearance of ray effect. It is important to note, however, that although both false scattering and ray effect can be lessened by increases in spatial grid size and angular directions or other means, they cannot be entirely eliminated according to numerical discretization nature.

A consequence of any method in which the continuous angular variation is discretized is that conservation of scattered energy may be violated after directional discretization. In order to ensure that the scattered energy is accurately conserved in the medium after DOM or TDOM discretization, the following relation must be satisfied for discrete direction $\hat{s}^{l'}$:

$$\frac{1}{4\pi} \sum_{l=1}^M \Phi^{l'l} w^l = 1. \quad (12)$$

This identity has shown to be exactly true only when the scattering is isotropic. When the scattering becomes highly anisotropic, however, this condition has been shown to be violated (Kim and Lee, 1988). In order to correct for the lack of conservation of scattered energy, phase function normalization is employed. Several publications (Wiscombe, 1976; Kim and Lee, 1988; Liu et al., 2002) have provided normalization schemes which will accurately satisfy Eq. (12). However, Boulet et al. (2007) showed that the previously published normalization techniques alter the overall asymmetry factor of the scattering phase function, leading to unrealistic and inaccurate intensity fields.

In order to correct for this problem, Hunter and Guo (2012a) proposed a new normalization technique which conserved both the scattered energy condition of Eq. (12) and the phase function asymmetry factor condition as follows:

$$\frac{1}{4\pi} \sum_{l=1}^M \Phi^{l'l} w^l \cos(\Theta^{l'l}) = g, \quad (13)$$

where the asymmetry factor g of the scattering phase function is a measure of the average cosine of scattering. The phase function is normalized in the following manner (Hunter and Guo, 2012a):

$$\tilde{\Phi}^{l'l} = \left(1 + A^{l'l}\right) \Phi^{l'l}, \quad (14)$$

where the normalization parameters $A^{l'l}$ are determined such that $\tilde{\Phi}^{l'l}$ satisfies Eqs. (12) and (13) simultaneously, while also satisfying the directional symmetry (i.e., $\tilde{\Phi}^{l'l} = \tilde{\Phi}^{l'l}$). The normalization parameters that will accurately satisfy the scattered energy and asymmetry factor constraints can be determined through pseudo-inversion.

It is important to note that normalization of the ballistic scattering phase function is independent of the previous normalization unless the direction of ballistic incidence directly matches one of the prescribed DOM discrete ordinate directions. Therefore, care must be taken to ensure that the ballistic phase function also satisfies the constraints on scattered energy and asymmetry factor. The ballistic scattering phase function can be normalized in a similar way to Eq. (14), in which the l' direction is replaced by l^b . In the case where the direction of ballistic incidence exactly matches a DOM ordinate, the parameters determined in Eq. (14) can be used to normalize the collimated scattering phase function.

3.3 Development and Applications of TDOM

Kumar and Mitra (1999) and Mitra and Kumar (1999) investigated and reviewed ultrafast radiation transport in a 1D planar medium subjected to a normal square-pulsed radiation beam. In their investigations, they compared transmitted and backscattered fluxes calculated using the DOM, two-flux method, and spherical harmonics methods. They determined that the different solution methods produced different effective propagation speeds, which significantly differed from the speed of light. As the number of discrete ordinates was increased, the effective propagation speed of the DOM approached the theoretical expectation, leading to more accurate transient flux measurements as compared to the other examined solution methods. Mitra and Churnside (1999) used the 1D TDOM as a method of detecting backscattering signals obtained from oceanographic lidar. They showed that the number density of fish and the depth of the "fish-layer" have a noticeable impact on backscattered signal peaks. Additional work by Sakami et al. (2002b) compared transmitted and reflected signals in a 1D planar tissue medium containing inhomogeneities irradiated with a short-pulsed laser using the DOM, as well as the parabolic diffusion approximation and the hyperbolic P_1 model. They found that while the solutions produced by the TDOM accurately match Monte Carlo results, the results from the hyperbolic P_1 and parabolic diffusion approximation produce unrealistic negative reflected signal values for short times due to the discrepancies in speed of propagation. A recent work considered the impact of variable medium refractive indices on transient radiant heat transfer (Wang and Wu, 2010).

The first 2D extension of the TDOM was performed by Guo and Kumar (2001a), in which ultrafast radiative transfer was determined for a rectangular enclosure subjected to diffuse and collimated laser irradiation. They indicated that, for long times, transient results show an excellent match with steady-state exact solutions for simple cases, and additionally verified the TDOM using Monte Carlo results. Along with developing the TDOM algorithm in 2D, they investigated USP laser transport in both homogeneous and inhomogeneous turbid media. They found that the TDOM correctly predicts that the ballistic component of laser propagates at the medium speed of light, with peak incident radiation value decreasing dramatically as it propagates deeper into the medium. Additionally, the diffuse com-

ponent of laser intensity propagates at a much slower speed, due to multiple-scattering events. They also discussed that distinct differences appear in transmittance and reflectance curves when comparing homogeneous and inhomogeneous media. Later, Sakami et al. (2002a) also developed the 2D TDOM with high-order upwind piecewise parabolic interpolation.

In 2002, Guo and Kumar (2002) published the first 3D TDOM, applying the method to determine ultrafast radiative transfer in a rectangular enclosure containing a nonhomogeneous medium. They established the model in full detail, validating the model by both comparing steady-state results to previously published benchmark cases and by comparing temporal distributions of transmittance and reflectance to those found using the Monte Carlo method. They performed an in-depth parametric study, investigating the impact of grid size, time step, boundary reflectivity, and optical properties. After fully developing the model, Guo and Kim (2003) investigated the light propagation and radiation transfer of ultrafast laser pulses in a 3D heterogeneous biological tissue sample. They noted that it was essential that the Fresnel boundary condition be imposed at the tissue/air interface in order to accurately predict photon transport in the tissue medium. In addition, they found that the peak positions of reflectance and transmittance are greatly influenced by the presence of inhomogeneity in the cubic enclosure, further validating the notion that changes in the absolute value of logarithmic slope of these quantities could be used to design a technique for imaging/detecting small tumors under the skin.

Kim and Guo (2004) extended the TDOM in 2004 for use in cylindrical geometries accommodating Gaussian laser beam distributions, analyzing ultrafast radiative heat transfer during laser welding and soldering processes and finding that the use of USP lasers decreases laser energy deposition in the proximity of the laser incident spot immediately after incidence, avoiding overcoagulation in the fusion area and allowing for better quality of closure. Further work by Kim and Guo (2007) combined the TDOM with a hyperbolic conduction heat transfer model to simulate many-time-scale heat transfer in turbid tissue exposed to USP irradiations. Ultrafast laser radiative transfer occurs on the pico/nano time scale, while bio-heat transfer due to conduction occurs on the micro/meso-time scale. Jiao and Guo (2009) applied the TDOM for determining heat transfer in a skin tissue cylinder containing a small tumor using a focused laser beam, finding that use of a focused beam can penetrate deeper into tissue and produce a higher temperature rise at the tumor location while reducing thermal damage to surrounding tissues, making focused ultrashort laser pulses an interesting alternative to killing cancerous tumors. They also demonstrated that the Beer–Lambert law could not be used for predicting laser transport in biological tissues including skins. Accurate radiative transfer modeling is mandatory. Jiao and Guo (2011) further combined ultrafast radiative transfer modeling and the ablation rate equation to investigate plasma formation

during plasma-mediated ablation of tissue, comparing their model with existing experimental and numerical data with good agreement.

Many researchers have performed experiments in conjunction with numerical modeling in order to characterize the validity of radiative transfer solutions. The works by Das et al. (2003) and Trivedi et al. (2005) investigated USP laser propagation through tissue phantoms with and without embedded inhomogeneities using an argon-ion mode-locked laser with a pulse width of 200 ps. They compared temporal transmittance and reflectance determined using the TDOM with experimentally measured optical signals taken from a streak camera, finding that the numerical and experimental predictions were in reasonable agreement with one another. Further works by Pal et al. (2006) and Jaunich et al. (2008) performed experiments on *in vitro* rat tissue samples to characterize light interaction with skin layers and associated thermal response, as well as *in vivo* imaging of anesthetized rats containing either tumor-promoting agents injected into skin tissue or mammary tumors. They compared the experimental changes in optical and thermal signal with numerical results and found excellent agreement.

While the TDOM suffers from ray effect and false scattering, as mentioned previously, a distinct advantage of the TDOM lies in the computational efficiency. The works by Mishra et al. (2006) and Hunter and Guo (2011) compared the radiative transfer solutions determined using the DOM with those determined using either the FVM or the Discrete Transfer Method (DTM). In all cases, they found that the transient heat flux profiles determined using various methods were accurate when compared with each other. However, both studies found that the solution times using the DOM were much less than when other methods were employed. Reductions in the computational time stem from the fact that the extra computational cost from integrating over a solid angle range inherent in the FVM does not appear in the DOM formulation (Hunter and Guo, 2011).

As previously mentioned, Hunter and Guo (2012a) investigated the impact of a lack of conservation of scattered energy and asymmetry factor after DOM discretization, finding that previous normalization techniques to satisfy only the scattered energy condition skewed the overall phase function asymmetry factor for highly anisotropic scattering media. An example of the lack of conservation of asymmetry factor after phase function normalization can be seen in Fig. 2, where using the common Henyey–Greenstein phase function approximation, discretized values of phase function are plotted for $g = 0.80$ and 0.95 , and compared with theoretical values. Discretized phase function values are presented using the old normalization technique of Kim and Lee (1988) which only considers Eq. (12), and Hunter and Guo's new technique (2012a) which incorporates both conservation conditions, Eqs. (12) and (13). It is easily seen that, for strongly forward scattering, the lack of incorporation of the conservation of asymmetry factor condition leads to skewed values of the discretized phase function. However, the values predicted using Hunter and Guo's new technique accurately conform to the theoretical phase

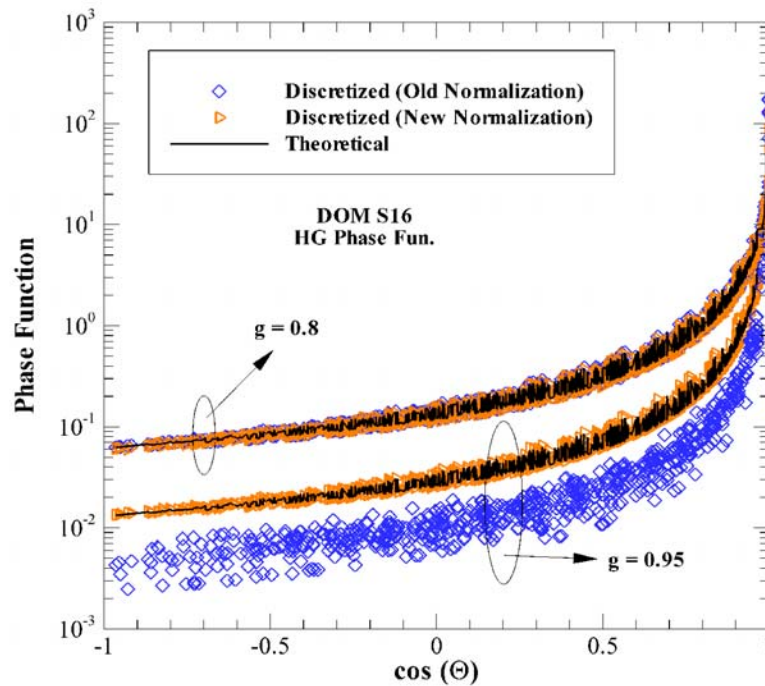


FIG. 2: Discretized phase function values vs. scattering cosine determined using varying normalization techniques for highly anisotropic HG scattering phase function [reproduced from (Hunter and Guo, 2012a)]

function values before discretization, indicating the necessity of ensuring that Eq. (13) is sufficiently satisfied.

The follow-up works by Hunter and Guo (2012b,c,d) investigated the impact of a lack of ballistic phase function normalization on radiative transfer solutions. As a means of validating the necessity for ballistic phase function normalization, radiative heat fluxes in a cold-walled, cubic enclosure containing a turbid media irradiated by a normal, collimated incidence at one wall generated using the DOM with S_{12} quadrature and ballistic phase function normalization are compared with benchmark Monte Carlo solutions (Collin et al., 2011) in Fig. 3. For strong-forward scattering, it is seen from Fig. 3 that the MCM and DOM solutions differ greatly (up to 34%) when no ballistic normalization is applied. When the old normalization technique is implemented, discrepancies are improved, but are not extremely accurate (differences of up to 13% witnessed). Application of the new Hunter and Guo technique dramatically improves the results when compared with MCM, leading to discrepancies of less than 1% at locations away from the cube wall. The discrepancies when either no normalization or the old normalization

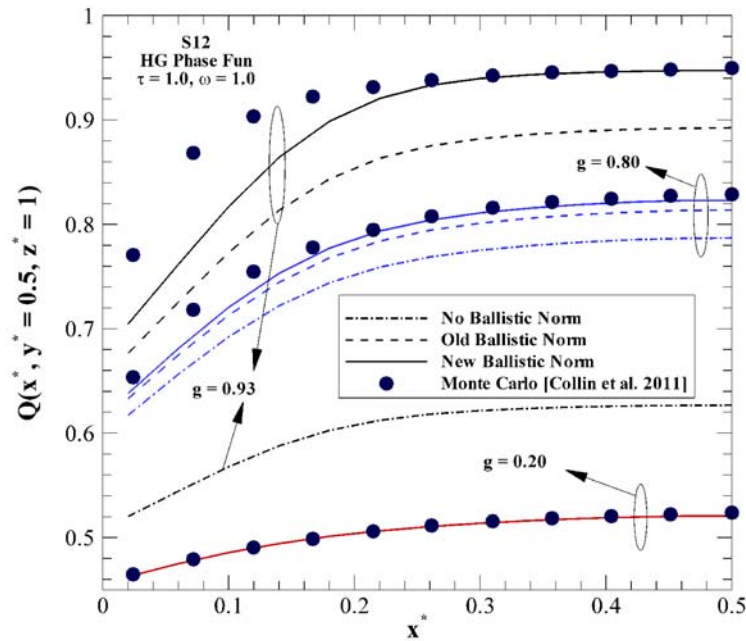


FIG. 3: Impact of ballistic phase function normalization on $Q(x^*, y^* = 0.5, z^* = 1)$ for normal, ballistic heating at $z^* = 0$ wall generated with DOM S_{12} for HG $g = 0.20, 0.80,$ and 0.93 and a comparison with Monte Carlo results (Collin et al., 2011) for optically thin medium [redrawn from (Hunter and Guo, 2012d)]

technique is applied are caused by lack of conservation of scattered energy and asymmetry factor for the ballistic phase function.

4. FINITE VOLUME METHOD

4.1 Governing Equations

The Finite Volume Method (FVM) was introduced as a method of solving the steady-state ERT by Raithby and Chui (1990), and expanded later on by Chui et al. (1992) and Chai et al. (1994) for various geometries. Similar to the DOM, the FVM employs a control-volume approach, discretizing the computational domain into arbitrary control volumes. The FVM employs the directional discretization of the 4π solid angle into a finite number of discrete solid angles, which completely fill the angular domain without overlap (Modest, 2002). The use of the control-volume approach for ERT discretization again allows the integro-differential source term to be approximated using a summation over a finite number of radiation directions (defined by the solid angles), thus greatly reducing the difficulty of solution.

Using the control-volume approach, the TERT is integrated over both an arbitrary control volume ΔV and discrete solid angle $\Delta\Omega^l$ (Chai, 2003). The discrete solid angle $\Delta\Omega^l$ is defined via azimuthal angle ϕ and polar angle θ , with discrete radiation direction \hat{s}^l denoting the centroid of the discrete solid angle (Murthy and Mathur, 1998; Chai 2004, Chai et al., 2004). Performing the aforementioned integration and applying Gauss' theorem to the integration of the spatial derivative, the TERT for a discrete radiation direction \hat{s}^l can be represented as follows:

$$\frac{1}{c} \frac{\partial}{\partial t} \int_{\Delta\Omega^l \Delta V} I^l dV d\Omega^l + \int_{\Delta\Omega^l \Delta A} I^l (\hat{s}^l \cdot \hat{n}) dV d\Omega^l = \int_{\Delta\Omega^l \Delta V} \beta (-I^l + S^l) dV d\Omega^l. \quad (15)$$

Evaluating the integrations over the control volume and solid angle, the TERT can be expressed in the form

$$\frac{1}{c} \frac{\partial I^l}{\partial t} \Delta V \Delta\Omega^l + \sum_i I_i^l A_i D_i^l = \beta (-I^l + S^l) \Delta V \Delta\Omega^l, \quad l = 1, 2, \dots, M, \quad (16)$$

where the area integration of the second term yields a summation over the faces i of the arbitrary control volume. In the aforementioned term, I_i^l represents the radiation propagating in the direction \hat{s}^l at the i th control-volume face; A_i is the surface area of the i th control-volume face, and D_i^l represents the directional weight of radiation direction \hat{s}^l at the i th control-volume face, represented by the following integral expression:

$$D_i^l = \int_{\Delta\Omega^l} (\hat{s}^l \cdot \hat{n}_i) d\Omega^l, \quad (17)$$

where \hat{n}_i is the unit vector normal to the i th control-volume face.

The source term S^l for a medium irradiated via an ultrashort pulsed laser can be expressed for a given radiation direction \hat{s}^l as follows:

$$S^l \cong (1 - \omega) I_b + \frac{\omega}{4\pi} \sum_{l'=1}^M \bar{\Phi}^{-l'l} I^{l'} \Delta\Omega^{l'} + \frac{\omega}{4\pi} \sum_B I^B \bar{\Phi}^{-lB}, \quad (18)$$

where $\bar{\Phi}^{-l'l}$ is the average scattering phase function between two discrete solid angles $\Delta\Omega^{l'}$ and $\Delta\Omega^l$, the necessity of which will be discussed in what follows.

4.2 Numerical Scheme

In order to determine the spatial and temporal intensity field in a general enclosure, Eq. (16) can be expanded over a generic control volume with the nodal center p . Using a forward-differencing technique for the temporal derivative and expanding over the aforementioned control volume, Eq. (16) can be expressed as

$$\frac{\Delta V \Delta\Omega^l}{c \Delta t} (I_p^l - I_p^{l0}) + \sum_i I_i^l A_i D_i^l = -\beta I_p^l \Delta V \Delta\Omega^l + \beta S_p^l \Delta V \Delta\Omega^l, \quad l = 1, 2, \dots, M. \quad (19)$$

The nodal intensities I_p^l are determined from the above equation in a control-volume marching scheme, similar to that outlined above for the TDOM. Equation (19) is more readily solved if the intensities I_i^l at the control-volume faces i can be related to the intensities I_I^l at neighboring control-volume nodal points I , due to the fact that the intensities at the upstream control-volumes nodes have already been determined using the marching scheme. There are many possible schemes to relate facial and nodal intensities (Modest, 2002). Commonly, a simple step scheme is implemented, due to the fact that I_p^l is guaranteed to remain positive.

Using the step scheme, the intensities entering the control volume at the upstream faces are set equal to the nodal intensities at the upstream control volumes ($I_i^l = I_I^l$), while the intensities leaving the control volume at the downstream faces are set equal to the current control-volume nodal intensity ($I_i^l = I_p^l$). Using the step scheme, Eq. (19) can be solved for I_p^l as follows:

$$I_p^l = \frac{\frac{\Delta V \Delta \Omega^l}{c \Delta t} I_p^{l0} + \beta S_p^l \Delta V \Delta \Omega^l + \sum_{i, D_i^l < 0} I_i^l A_i |D_i^l|}{\frac{\Delta V \Delta \Omega^l}{c \Delta t} + \beta \Delta V \Delta \Omega^l + \sum_{i, D_i^l > 0} A_i D_i^l}. \quad (20)$$

The equations presented here are given for general control volumes and geometries, with more complete details available in Chai et al. (2004) for three-dimensional Cartesian geometries and in Hunter and Guo (2011) for an axisymmetric cylindrical medium. As noted for the TDOM, it is essential that the traveling distance of light does not exceed the minimum size of a given control-volume in any direction.

A distinct advantage of the FVM over the DOM lies in its inherent flexibility of directional choice. While the discrete directions in the DOM must satisfy the given moment constraints, the radiation directions (i.e., solid angles) in the FVM can be chosen arbitrarily (Chai et al., 1994; Murthy and Mathur, 1998; Chai, 2004; Chai et al., 2004). Although unstructured discretization of the angular variation is possible (Murthy and Mathur 1998), it is common to adopt structured discretization, with the total solid angle of 4π divided into $(N_\phi \times N_\theta)$ equally spaced solid angles, with N_ϕ divisions in the azimuthal direction and N_θ divisions in the polar direction. It has been found, however, that the FVM does still suffer from ray diffusion (false scattering) and ray concentration (analogous to ray effect in the DOM) errors, as reported by Raithby (1999), due to the spatial and angular discretization inherent in the FVM.

In the source term of Eq. (18), an average scattering phase function $\overline{\Phi}^{l'l}$ is used to calculate the change in intensity due to in-scattering. The necessity of using this average scattering phase function stems from the need to accurately conserve the scattered energy after directional discretization. The scattered energy conservation constraint for the FVM is initially equivalent to Eq. (12) given above for the

DOM, only with quadrature weight w^l replaced by the discrete solid angle $\Delta\Omega^l$. As in the DOM, this condition is only exactly satisfied after directional discretization if scattering is isotropic. In order to correct for a lack of scattered energy conservation, when scattering is anisotropic, Raithby and Chui (1990) introduced a technique by which the discrete solid angles $\Delta\Omega^l$ and $\Delta\Omega^{l'}$ are further split into numerous subangles $\Delta\Omega^{l_s}$ and $\Delta\Omega^{l'_s}$. The scattered radiant energy calculated between the subangles is averaged to determine the total scattered energy between discrete solid angles $\Delta\Omega^l$ and $\Delta\Omega^{l'}$.

While the scattered energy condition is conserved accurately when the solid angles are split into a large enough number of subangles, Hunter and Guo (2012e) found that the subangle procedure does not accurately conserve the asymmetry factor condition in the system, i.e., Eq. (13) is not accurately satisfied, even for an extremely fine solid-angle splitting grid. In order to ensure that both the scattered energy and asymmetry factor conditions are satisfied simultaneously, the phase function normalization procedure of Eq. (14) given above can be implemented. Not only does the normalization procedure accurately conserve both the scattered energy and asymmetry factor, it also reduces the need to split each solid angle into numerous subangles in order to obtain accurate intensity fields. The use of normalization combined with minimal solid-angle splitting provides accurate intensity fields and drastically increases computational efficiency (Hunter and Guo, 2012e).

4.3 Development and Applications of the FVM for Ultrafast Radiative Transfer

The first use of the FVM to solve the TERT is found in Chai (2003), in which radiative transfer in a one-dimensional slab was investigated. In addition to building the framework for the FVM in ultrafast radiative transfer, Chai validated the FVM results by comparing them with previously published results determined using the integral method. He also examined the impact of both the step and Curved Line Advection Method (CLAM) high-resolution spatial differencing schemes on test problems including irradiation of a slab with either a single-pulse or repeated-pulse collimated beam. He concluded that in order to accurately predict the sharp discontinuities inherent in a collimated laser incidence, a higher-order bounded spatial differencing scheme such as the CLAM scheme is necessary. In a follow-up work, Chai (2004) extended the use of the FVM for ultrafast radiative transfer in 2D rectangular geometries, finding excellent agreement with Guo and Kumar's TDOM results (2001a) for an anisotropically scattering medium in a square enclosure.

An extension to three-dimensions was presented by Lu et al. (2003) and Chai et al. (2004). In these works, the results from the FVM were compared to the previously published results using the integral method of Tan and Hsu (2002) for a black cubic enclosure with one hot wall containing an absorbing and isotropically

scattering medium. The step and CLAM schemes were again compared with similar results for the 1D and 2D cases described above. Although the CLAM scheme was shown to predict the penetration depth and steep gradients of intensity better than the step scheme, discrepancies were seen when compared with the integral method. Lu et al. (2003) found that the false-scattering inherent in the FVM method introduced discrepancies in both the peak intensity value and penetration/decay time, noting that neither spatial differencing scheme was able to recover the correct propagation speed, which becomes significant for optically thick media.

Later, Muthukumaran and Mishra (2008b) investigated the interaction of a single-pulse and 4-pulse train with the Gaussian temporal profile in a 1D plane-parallel inhomogeneous medium made up of layers with varying optical properties. Muthukumaran and Mishra (2008a) extended their study to two dimensions, investigating the transient transport of a train of USP collimated incident radiation through a 2D rectangular participating medium with and without inhomogeneities. Muthukumaran et al. (2011) analyzed the transport of a short-pulsed laser with both a step and Gaussian profile through a human tissue phantom. The laser pulse width was varied between ns, ps, and fs, and the medium was taken to be either homogeneous or inhomogeneous. They determined that the peak magnitudes of transmittance were comparable for the ps and fs temporal span, but differed by multiple orders of magnitude for the ns case. They also determined that the peak reflectance signal between the ps and fs cases differed by seven orders of magnitude, illustrating the importance of laser pulse width.

Recently, Rahmani et al. (2009) investigated the prediction of ultrafast radiant energy transfer with the FVM using a generalized computational grid, introducing a new method to treat the control angle overhang. Asllanaj et al. (2007) solved for ultrafast radiative transfer in a 2D complex shaped domain using unstructured triangular meshes with the FVM using a cell vertex scheme, validating their results with benchmark cases. Kim et al. (2010) solved for ultrafast radiative transfer in a 1D planar medium subjected to radiative equilibrium. Many previous studies on ultrafast radiative transfer assumed the medium to be either cold or at a constant temperature. Kim et al. (2010) argued that, for applications such as the short-pulse heating of metals, irradiated radiant energy increases the medium temperature throughout the entire process, causing differing temporal and spatial thermal behavior inside the medium. They reiterated the necessity of using a high-order convection scheme to accurately capture the wave front discontinuity for collimated irradiation. For the medium subjected to radiative equilibrium, the temporal evolution of incident radiation is more pronounced than for the cold medium, and the radiative heat transfer in the medium converges to a constant value throughout, unlike the case where the medium is cold or at a constant temperature. Ruan et al. (2010) performed an analysis of transient radiative transfer in a 1D inhomogeneous layered media irradiated by a short-pulsed laser, witnessing a "dual-peak" in the reflectance signals due to the inhomogeneity of the participating media. Padhi et al. (2011) investigated the short-pulsed laser irradiation of a 2D partici-

pating medium with diffusely reflective boundaries, finding that the "dual-peak" reflectance phenomenon vanishes with increase in both the optical thickness and wall emissivity.

While the FVM offers the flexibility of both angular and spatial discretization, the integration over the 4π solid angle causes a decrease in computational efficiency over the DOM. Mishra et al. (2006) verified that the FVM was not as computationally efficient as the DOM, but showed that the FVM is still more computationally efficient than the procedures that perform ray tracing, such as the DTM. Hunter and Guo (2011) compared the FVM with DOM for both steady-state and ultrafast radiative transfer analyses in absorbing and isotropic scattering media. They showed that, for an axisymmetric cylindrical medium, the FVM without angle splitting took up to 1.15 times longer to converge for optically thick, purely scattering media than the DOM. In addition, the computational memory usage by the FVM was also larger than that by the DOM. For highly anisotropic scattering, however, solid-angle splitting is needed in order to satisfy the conservation of scattering energy. This will increase substantially the overall computational time for the FVM. Use of appropriate phase function normalization technique would reduce the level of required angle splitting (Hunter and Guo, 2012e), and thus lessen the increased FVM computational time with angle splitting. Figure 4 displays both CPU convergence time and convergence time ratios of nonnormal-

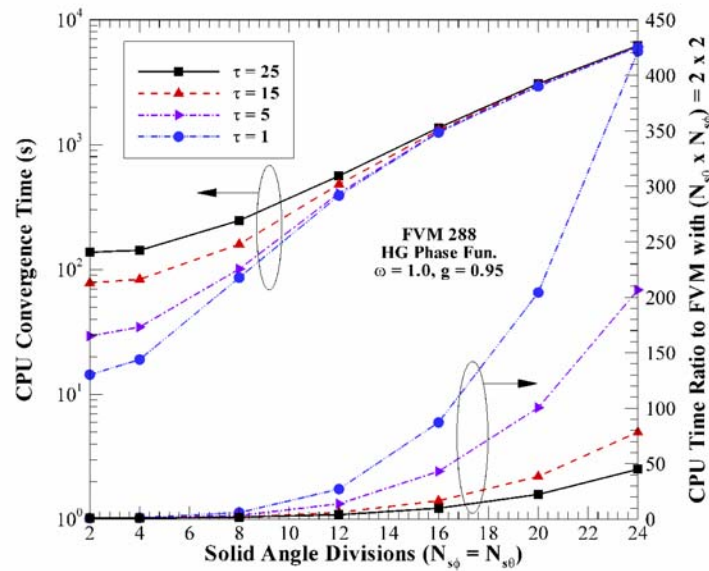


FIG. 4: CPU convergence times with varying angle splitting and convergence time ratios of non-normalized FVM with varying solid-angle splitting to normalized FVM with $(N_{s\phi} \times N_{s\theta}) = 2 \times 2$ splitting [reproduced from (Hunter and Guo, 2012e)]

ized FVM with varying levels of solid-angle splitting to the normalized FVM with $(N_{s\phi} \times N_{s\theta}) = 2 \times 2$ angle splitting for varying optical thickness with $g = 0.95$ (Hunter and Guo, 2011e). It is seen that the CPU time ratio between the $N_{s\phi} \times N_{s\theta} = 24 \times 24$ and 2×2 cases is extremely large. For the optically thick medium ($\tau = 25$), the 24×24 case takes 45 times longer to converge than the 2×2 case. The ratio increases dramatically with decreasing optical thickness. This illustrates the advantage of using phase function normalization for the FVM. Not only the scattered energy and asymmetry factor are explicitly conserved, but the convergence time is decreased by a few orders of magnitude when compared to the non-normalized convergence time with a large number of split subangles.

5. MONTE CARLO METHOD

Accurate treatment of the integro-differential term in the ERT can be a formidable task. Deterministic methods, such as the DOM and FVM, are able to treat this term fairly accurately with a sufficient number of discrete radiation directions. As previously discussed, however, use of a finite number of radiation directions to approximate the full 4π solid angle introduces numerical error due to ray effect, and spatial discretization induces numerical diffusion. In addition, it can be extremely difficult to solve the ERT for realistic situations involving complex physical geometries. These issues can be avoided through the use of the Monte Carlo Method (MCM). A major advantage of the MCM is that it can handle almost all physical and geometrical conditions, including such as anisotropic scattering, Fresnel reflection, and refraction; and thus, is sometimes considered as an alternative to realistic experiments. While the MCM provides a relatively simplistic manner of solution for radiative transfer, it suffers from two well-known shortcomings: statistical errors and computational inefficiency.

MCM algorithms for steady-state radiative transfer predictions can be found, in great detail, in the textbook of Howell et al. (2010), and thus are not repeated herein. When ultrafast radiative transfer is concerned, the solution algorithm does not change except for the incorporation of photon flight time (Guo et al., 2000, 2002). As described in Guo et al. (2000), the initial photon emission time can be determined through the use of random numbers, and the total time of flight of an individual photon before experiencing absorption or scattering events is directly related to the optical path length through the medium speed of light. By calculating the photon flight time, MCM simulations can be performed until the total flight time reaches a certain predetermined limit, or until photons either escape the medium boundaries or lose a certain amount of energy due to medium interaction. Duhamel's superposition theorem can also be used to construct the response of a single pulse or pulse train from the MCM response to an impulse irradiation in which the initial photon emission time is null (Guo et al., 2002).

Jacques (1989) was one of the first to consider the MCM as a method of investigating time-resolved ultrashort laser propagation in a turbid tissue. In his work,

Jacques investigated internal fluence distribution and propagation depth due to both impulse and pulsed laser incidence at the tissue surface for varying tissue optical properties. He found that, for fs pulses, two photon reactions were dominated by the initial unaltered incident pulse, while single photon reactions were dominated by the diffuse scattered irradiance. When ps pulses were investigated, it was found that both reactions were dominated by diffuse scattered incidence due to the fact that the scattered light accumulated near the surface and exceeded the irradiance of the primary pulse. When investigating the impact of medium anisotropy, it was found that the primary laser pulse penetrated further into the tissue medium than expected based on the knowledge of the medium extinction coefficient for strong-forward scattering.

Hasegawa et al. (1991) used the MCM to simulate the variation of temporal transmittance in a slab of particles in order to verify and explain the microscopic Beer–Lambert law. In their model, the slab contained both isotropically scattered particles and either a pigment or strongly-forward scattering particles irradiated by a collimated light source that was taken to either be an impulse or Gaussian profile at 10 ps FWHM. They determined, through investigation of temporal transmittance, that differences in the optical density among slabs with different absorption coefficients but equal scattering coefficients vary linearly with time, thus verifying the applicability of the microscopic Beer–Lambert law. They also compared the MCM to the DA, confirming that the DA is only valid for the time long after the initial incidence and for locations far from the incidence point. Hielscher et al. (1996) investigated time-resolved photon emission profiles from layered turbid media with the MCM, comparing the numerical solutions with experimental measurements on gelatin tissue phantoms. They found that MCM results accurately conformed to the experimental results tested, finding that it was possible to use time-resolved reflectance measurements to determine the absorption coefficients of tissue layers that were not adjacent to the incident surface.

Guo et al. (2000) applied the MCM for determining 2D ultrafast radiative transfer, investigating an absorbing and scattering medium irradiated by a spatial and temporal Gaussian pulsed laser. They investigated the influences of anisotropic scattering, incident pulse width, and the impact of the including of a Fresnel reflection boundary condition for refractive index change. The results showed that including Fresnel reflection at boundaries where the refractive index changes occur was crucial for accurate prediction of transmittance and reflectance profiles, while the medium dimensions were shown to significantly impact the log-slope of reflectivity, mandating the necessity for performing multidimensional simulation. An additional work by Guo et al. (2002) expanded the use of the MCM for determining ultrafast radiative transfer in a 3D enclosure and compared the MCM simulation with experimental measurements. Figure 5 shows the comparison of the temporal transmittance profiles via MCM simulation of anisotropic scattering and experimental measurements for a 60-ps pulse at wavelength 532 nm passing through a

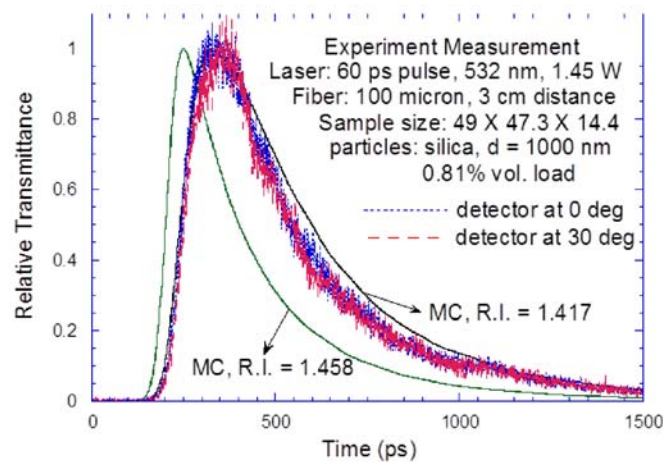


FIG. 5: Comparison of MCM simulation with experimental measurement [reproduced from (Guo et al., 2002)]

3D block of 14.4-mm thickness containing 0.81% silica microparticles. The refractive index (R.I.) of material determines the optical properties. The R.I. of silica is 1.417 at wavelength 550 nm and 1.458 at 589 nm. At R.I. = 1.417, the scattering coefficient is determined to be 17.052 mm^{-1} with an asymmetry factor of $g = 0.96276$. From the figure, it was found that the angle of transmittance had no noticeable impact on the shape of hemispherical transmittance profiles and the predicted profile by MCM with R.I. = 1.417 matched well with the experimental measurements.

Guo and Kumar (2000) determined that the use of the isotropic scaling law (Lee and Buckius, 1982; Guo and Maruyama, 1999) was not able to produce accurate transient results for ultrafast radiative transfer analysis. Figure 6 compares the temporal profiles of transmittance and reflectance for various scattering media subjected to a collimated irradiation. All the media have an equivalent isotropic scattering coefficient (sometimes called as reduced scattering coefficient). It is seen that the scaled isotropic scattering results do not match well with the anisotropic scattering results at the early time stage. For backward scattering media, the scaled isotropic result cannot capture the peak; while for forward scattering, the scaled isotropic result will overpredict the peak. Unfortunately, most of the work on light scattering in highly anisotropically scattering biological tissues adopted the concept of reduced scattering coefficient.

A work by Wong and Menguc (2002) investigated the propagation of a collimated beam in a plane-parallel participating media using three different MCM approaches, which differed in their treatment of the photon interaction distance. The first method (MCM1) calculated a single interaction distance based on the medium

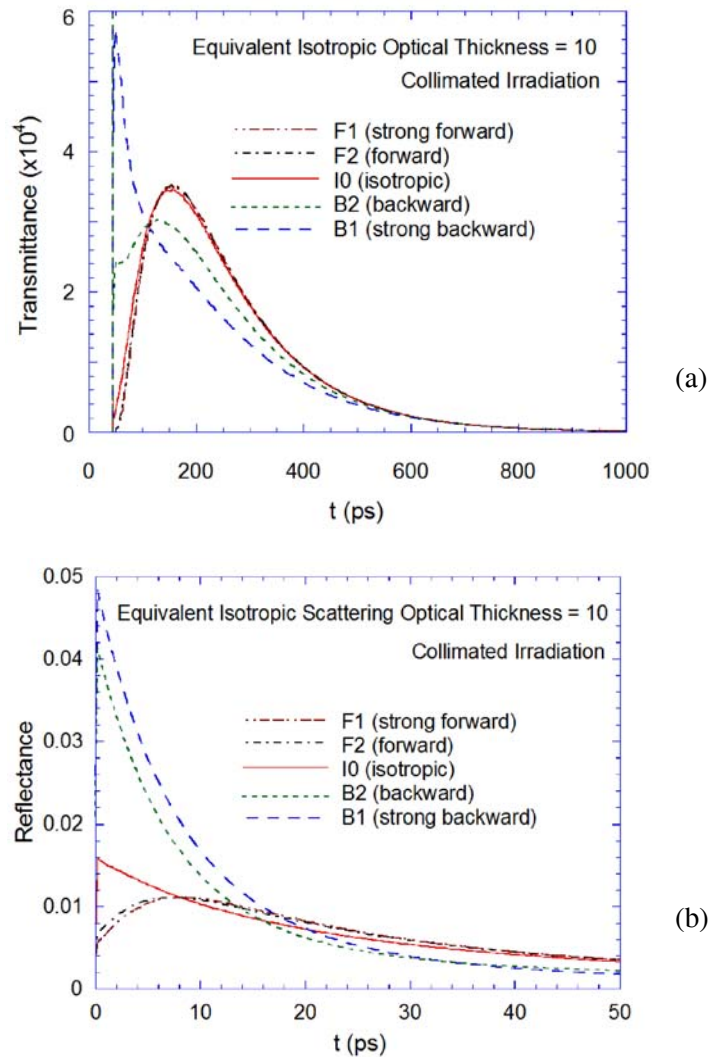


FIG. 6: Comparison of temporal distributions of (a) transmittance and (b) reflectance for various scattering media of equivalent isotropic scattering effect [reproduced from (Guo and Kumar, 2000)]

extinction coefficient. The second method (MCM2) used the scattering coefficient to calculate the interaction distance, and the third (MCM3) took into consideration two separate interaction distances for absorption events and scattering events. They determined that each individual method had ranges of optical properties in which they were preferred for predicting transmittance and reflectance, based on the changes in statistical variance. While they did not report absorption profiles, they

mentioned that MCM1 and MCM3 yield identical absorption profiles, while predictions from MCM2 are more time consuming.

There have been many additional applications of the MCM in recent years. Wu (2009) investigated ultrafast radiative transport in a refractive planar medium exposed to collimated irradiation. The time of flight of the photons was derived for a medium with a linearly varying refractive index. They found that the MCM results conformed accurately to those determined using the DOM, and that continuous variation of refractive index in a medium has a significant impact on ultrafast radiative transfer, including the decrease in reflectance and appearance instant of transmittance peak with refractive index increase. Sawetprawichkul et al. (2002) investigated 3D transient radiative transport using the MCM via parallel computation to improve computational efficiency. Wan et al. (2004) investigated the non-invasive detection of inhomogeneities, such as tumors, in turbid media using log-slope analysis of back-scattered intensity, validating their technique with both experimental results and MCM simulations. Additionally, Guo et al. (2006) used the MCM as a method to simulate light transport and signal measurement in order to examine a novel optical temporal log-slope difference mapping approach for imaging of cancerous breast tumor.

As stated earlier, the main drawback of the MCM lies in the computational time, as extremely large numbers of photons must be traced from emission to absorption points in order to determine suitable statistical averages for intensity and heat flux. In order to alleviate the computational drawbacks, Lu and Hsu (2004) introduced a reverse MCM for determining transient radiative transfer in participating media. In this method, photon bundles are tracked in a time-reversal manner from the point of absorption back to emission from the detector site. This method is claimed to be more computationally efficient than the conventional MCM, due to the fact that it is not necessary to track photons that never reach a collector site. However, this procedure will generate less information about transport processes, due to the fact that information is only obtained at specific detector locations, meaning that it may not be appropriate for situations where detailed information is required about the transient transport process. Follow-up works by the same authors investigated light pulse propagation in nonhomogeneous media (Lu and Hsu, 2005) and a medium containing highly scattering embedded cores (Hsu and Lu, 2007), finding good agreement between conventional MCM and reverse MCM results.

6. OTHER METHODS

While the four methods previously mentioned are among the most popular thus far, there are several other numerical methods to determine ultrafast radiative transfer via solution of the TERT. The Radiation Element Method (REM) (Guo and Kumar, 2001b; Guo et al., 2001) was developed for ultrafast radiative transfer modeling in 2001. REM is a generalized zonal method, in which the governing

equation is integrally solved and ray-tracing is employed to determine radiant-energy fraction-based view factors (Maruyama and Aihara, 1997). Since the time dependence is an integral solution, this method can capture exactly the propagation speed of light, eliminating numerical diffusion associated with discretization-based methods like DOM and FVM. However, this method is relatively difficult to implement. The DTM (Mishra et al., 2006), introduced by Rath et al. (2003) for ultrafast radiative transfer in 2003, is an approximate method that combines the use of discrete directions with a ray-tracing procedure. The P_N spherical-harmonics method (Mitra et al., 1997; Wu and Bhuvaneshwari, 2009) eases the TERT solution by transforming the integro-differential equation into a set of partial differential equations, with the P_1 approximation leading to the diffusion equation, as discussed earlier. The Modified Method of Characteristics (Katika and Pilon, 2004) transforms the TERT into an ordinary differential equation along photon pathlines. To reduce the errors inherent in the approximate solution methods, the Integral Method (IM) (Wu and Wu, 2000; Tan and Hsu, 2002) was implemented. In this method, the TERT is directly integrated based on geometric constraints, eliminating ray effect and numerical diffusion errors for cases where the medium geometry is not too complex.

Table 1 lists comparisons of CPU convergence times for different numerical schemes (DOM, FVM, DTM, DA, and MCM) available in the literature. It is important to note that CPU convergence times for each scheme are highly dependent on the exact problem studied (boundary conditions, medium optical properties), computational parameters (spatial and temporal grid size, number of rays/directions) and the computational workstation itself (amount of RAM, processor speed, etc.). While the values listed for each specific problem cannot be directly compared to other problems, generalizations in computational time can be made between specific numerical methods. The DOM and FVM approximate methods tend to converge much more quickly than the DTM, which implements computationally intensive ray tracing. The MCM has extremely large computational time in comparison, due to complex ray tracing and statistical averaging requiring multiple simulations. Use of the DA greatly reduces computational time as compared to the DOM, due to the reduction of the integro-differential ERT into a simplified set of partial differential equations. In general, the DA will have the lowest computational time, and the MCM will have the highest, due to the specific nature of the methods.

7. SOME BIOMEDICAL APPLICATIONS

The advent and subsequent development of ultrafast laser technology has allowed for significant advances in the field of biomedicine. This section reviews some applications in which accurate modeling and understanding of ultrafast laser transport and/or interaction with biological tissues is critical.

TABLE 1: Comparison of computational times for various numerical methods

Source	Computational time (min)				
	DOM	FVM	DTM	DA	MCM
Mishra et al. (2006) ^a	5.48	6.35	8.95	–	–
Mishra et al. (2006) ^b	10.3	15.4	16.0	–	–
Mishra et al. (2006) ^c	1.43	2.60	2.76	–	–
Hunter and Guo (2011) ^d	6.61	7.47	–	–	–
Hunter and Guo (2011) ^e	0.38	0.42	–	–	–
Guo et al. (2003) ^f	480	–	–	60.0	–
Henson and Malalasekera (1997) ^g	–	–	0.83	–	410
Henson and Malalasekera (1997) ^h	–	–	4.08	–	49.1

^a 1D planar, cold medium subject to short-pulsed collimated irradiation, unity optical thickness, black boundaries. 500 control volumes, 10 directions. IBM Thinkpad Model R40, Pentium 4 2.0 GHz with 256 MB RAM

^b Case a, except with 40 directions

^c Case b, except with 100 control volumes

^d 2D axisymmetric. cylindrical enclosure containing cold, absorbing/emitting/isotropic scattering medium w/diffusely emitting hot side wall, optically thick ($\tau = 5.0$), purely scattering. (150×150) mesh, 288 directions — Dell Optiplex 780 w/Intel 2 Dual Core 3.16 GHz, 4.0 GB RAM

^e Case d, except optically thin ($\tau = 0.1$)

^f 3D cubic enclosure — participating media of base tissue (highly scattering), with tumor inhomogeneity of differing absorption coefficient. Medium irradiated by 60 ps short-pulsed laser at boundary with Gaussian profile, staggered ($27 \times 27 \times 27$) computation grid. DOM S10 (120 directions), $\Delta t = 4$ ps. DA approximation using FEMLAB w/ 10^4 finite elements

^g 3D unit cube enclosing isothermal, absorbing, emitting, isotropically scattering medium with cold/black walls. ($9 \times 9 \times 9$) orthogonal mesh, purely absorbing ($\tau = 0.0$), variable optical thickness. HP-9000/750 machine. MCM time for 30 simulations, 9.95×10^7 energy bundles. DTM using 400 solid angles per subsurface.

^h Case g, except $\omega = 0.90$, MCM bundles: 1.062×10^7 .

A particular application where ultrafast lasers have played an indispensable role is near-infrared optical imaging (Liu et al., 1993; Yoo and Alfano, 1993; Gu and Sheppard, 1995; Hielscher et al., 1995b; Yamada, 1995; Yodh and Chance, 1995; Alfano et al., 1997; Villringer and Chance, 1997; Quan and Guo, 2004) of foreign growths embedded inside biological tissue, such as cancerous tumors. Before the development of the aforementioned technology, imaging of inhomogeneities had been attempted using conventional approaches with CW light sources. However, the highly scattering nature of biological tissue made this difficult, as the shadows

caused by the inhomogeneities were washed out by the multiple random scattering of light (Liu et al., 1993). When ultrafast laser light penetrates into a biological tissue, it may be effectively split into a ballistic component, a diffuse component, and a snake component (Yoo and Alfano, 1993). The ballistic and snake components reach the inhomogeneity much earlier than the diffuse component, which undergoes multiple scattering events. As such, sophisticated time-resolved imaging techniques or coherent optical tomography can be used to detect the ballistic and snake components, which both illuminate and carry optical information about the growth, without detecting the multiple-scattered light that would wash out the overall image. A theoretical investigation performed by Gu and Sheppard (1995) reported nontrivial increases in the 3D image resolution using ultrafast laser light as compared with CW laser illumination at a given wavelength. When the medium is very turbid, such that diffuse radiation predominates, diffuse optical tomography was proposed (Ntziachristos et al. 2000) in which an inverse image reconstruction is conducted based on experimental measurements and continuous forward modeling of photon migration with testing optical properties (Yamada, 1995; Yodh and Chance, 1995). Inverse optimization techniques can be extremely time consuming, and to this end Guo et al. (2006) introduced a simple image-projecting method for initial screening that avoids such time-consuming techniques.

A study by Wang et al. (1991) achieved submillimeter image resolution during imaging of objects embedded behind various scattering walls, including human and chicken breast tissue, by implementing an ultrafast optical shutter and an imaging procedure that separated and rejected scattered diffusive light from the ballistic component. Zaccanti et al. (1992) carried out experimental measurements of light pulse transmission through thick turbid media using picosecond laser pulses, indicating that the properties such as the absorption coefficient could be obtained from pulse shape. In addition, they indicated the potential for detecting highly absorbing structures using time-gated scanning imaging techniques. Alfano and co-authors (Liu et al., 1993; Yoo and Alfano, 1993) further implemented ultrafast time-gated optical detection techniques to locate both translucent and opaque inhomogeneities embedded in thick tissue by isolating the early-arriving ballistic portion of ultrafast laser light. In a subsequent work, Alfano et al. (1998) reviewed several methods for extracting image-bearing light and investigated nonlinear optical tomography of human organs, indicating the potential for the development of safe and inexpensive diagnostic imaging techniques using near-infrared optical imaging with ultrafast laser technology.

Villringer and Chance (1997) investigated the noninvasive assessment of human brain activity *in vivo* using near-infrared light, detailing various additional applications for near-infrared spectroscopy and imaging, such as bedside monitoring cerebral oxygenation in patients at a risk of stroke. Benaron et al. (2000) additionally investigated optical imaging applications for monitoring human brain activity, ana-

lyzing photon transit time through the skull and brain tissue in order to achieve tomographic imaging of cerebral hemoglobin oxygenation and similarly stressing the ability of this technique for real-time clinical monitoring of oxygenation at bedside. Wu et al. (1997) presented a multichannel tomographic technique in order to detect fluorescent objects embedded in a thick turbid media, making use of early-arriving photons from picosecond laser pulses. They achieved submillimeter accuracy and millimeter resolution, indicating the feasibility of tomography for tumor detection in human breast tissue. Schmidt et al. (2000) additionally explored multichannel time-resolved imaging for the medical optical tomography, using the aforementioned technique to detect small inhomogeneities embedded in tissue phantoms.

Diffuse optical tomography of human breast tissue *in vivo* was performed by Ntziachristos et al. (2000), who obtained images after administering indocyanine green (ICG) and finding accurate results when compared to concurrently administered magnetic resonance imaging. Studies by Tromberg et al. (2000) and Hebden et al. (2001) additionally implemented diffuse optical tomography for imaging in breast tissue using picosecond laser pulses. More recently, Quan and Guo (2004) developed a fast 3D optical imaging method using an exogenous fluorescence agent. Using this technique, laser pulses excite fluorescence, allowing for the 3D image reconstruction of relative fluorescence distribution. They demonstrated the ability of this method for the accurate image reconstruction of a small tumor buried in turbid tissue.

Another application in which ultrafast laser technology has become indispensable is precise material removal and microprocessing via plasma-mediated ablation (Niemz et al., 1991; Loesel et al., 1998; Kim et al., 2001; Huang and Guo, 2009a; Guo et al., 2010; Wang and Guo 2010). The prediction of laser fluence for determining the optical breakdown threshold or temperature rise for material evaporation requires the knowledge of laser radiative transport in tissue (Jiao[Q5] and Guo, 2011). During plasma-mediated ablation, thermal diffusion to surrounding material is limited/eliminated, due to the fact that the material thermal relaxation time is much longer than the timescale of plasma formation due to laser-material interaction (Huang and Guo, 2009b; Huang and Guo, 2010). This phenomenon allows for material removal with an effective minimization of thermal damage to the surroundings, which is extremely important for applications involving biological tissue *in vivo*, as excessive thermal damage can lead to tissue necrosis. Previous use of CW laser light for effective cell removal led to somewhat extensive thermal and mechanical damage to the surrounding tissue (Niemz et al., 1991; Kautek et al., 1994), indicating the necessity for ultrafast laser technology.

Niemz et al. (1991) performed an early study of plasma-mediated ablation, investigating the impact of picosecond pulses on human donor corneas. They measured energy densities and mean tissue removal rate, and found the laser excisions to be smooth with minimal distortion. In addition, they introduced a quantitative

model for plasma-mediated ablation, finding it to be accurate with the results observed, indicating that mode-locked Nd:YLF lasers could be a feasible alternative to excimer lasers for corneal surgery. High-quality corneal tissue ablations were also achieved by Kautek et al. (1994) using femtosecond laser pulses. When compared with ablations performed using nanosecond pulses, they found thermal damage and tissue disruption to be greatly reduced. Both Fischer et al. (1993) and Loesel et al. (1998) investigated picosecond-pulsed ablation of human brain tissue, indicating that no thermal damage to the surrounding tissue was induced. Oraevsky et al. (1996) demonstrate the ability of ultrafast lasers to act as precise microsurgical tools, investigating femtosecond-pulsed plasma-mediated ablation of biological tissue and finding that high-quality ablation craters were obtained with no damage to the surrounding material. Feit et al. (1997) presented a detailed numerical modeling of the relevant physics behind ultrashort-pulsed laser ablation of biological tissue. Additionally, Kim et al. (2001) investigated ablation characteristics for pulse widths in the femtosecond and picosecond regime, observing differences in the ablation crater morphology for various pulse widths. Lapotko et al. (2007) studied cellular response to laser heating, building a model of laser radiation-cell interaction and comparing this model with experiment in order to more accurately gain information on cellular heat processes.

Works by Huang and Guo (2009a, 2010) were able to achieve thin-layer separation of both *in vitro* wet (Huang and Guo, 2009a) and freeze-dried human dermis (Huang and Guo, 2010) using USP lasers. They found that single line ablation resulted in no thermal damage to the surrounding material, and that multiline ablation caused minimal and insignificant thermal damage. Further works by Guo and co-authors (Guo et al., 2010; Wang and Guo, 2010) demonstrated the ability to separate and remove thin layers of biofilm contamination, removing contaminating layers of blood from various substrates using picosecond laser ablation. They found that this technique was able to effectively and neatly remove the biofilm contamination from the substrate without experiencing thermal diffusion damage.

The use of the thermal mechanism of ultrafast lasers to destroy cancerous tumors has also been investigated recently. Biological tissue responds very strongly to a temperature rise, and it additionally has been noted that cancerous tumor cells are much more sensitive to temperature increase than healthy tissue (Anghileri and Robert, 1986). Thus, by raising the temperature in cancerous tissue above a certain threshold, while maintaining safe temperature levels in surrounding healthy tissue, cancerous tumors can be effectively treated in cases where surgery is complicated or dangerous (Jaunich et al., 2008; Jiao and Guo, 2011). This process is known as the laser-induced hyperthermia (Anghileri and Robert, 1986). Use of ultrafast lasers with the beam focused at the tumor location allows for large temperature increase at the tumor location while minimizing temperature rise at surrounding healthy tissues (Jiao and Guo, 2011). This results in a minimization of the thermal

damage of healthy tissue and necrosis over previous attempts with CW lasers, making focused beam technology an ideal method for combating cancerous cells (Jiao and Guo, 2011).

Additional applications for ultrafast laser technology with regard to biomedicine include precise and minimally invasive laser microsurgery (Anderson and Parrish, 1983; Abergel et al., 1986; Arkin et al., 1994; Lubatschowski et al., 2003; Ridouane and Campo, 2006) and laser-tissue welding (Murray et al., 1989; Bass and Treat, 1995; Fried et al., 1999; Kim and Guo, 2004). Laser microsurgery is performed in many different areas of human body. Corneal surgery such as LASIK, which uses laser technology to permanently change corneal shape as a means of vision correction, uses femtosecond pulses in order to increase both speed of operation and surgical precision (Lubatschowski et al., 2003). A work by Ridouane and Campo (2006) investigated numerical computation of temperature evolution in the human eye during corneal refractive surgery, investigating sensitivity in corneal temperature distribution in order to accurately predict heat transmission during surgery. Laser tissue welding, a procedure by which tissues are bonded together using laser-activation of photothermal/photochemical bonds, has become a realistic alternative to other wound-closure methods, including sutures or staples, which can lead to scarring.

The biomedical applications of ultrafast lasers listed in this work are not exhaustive. However, the extensive use of ultrafast lasers in biomedicine in recent years indicates the overall power and importance of advances in this technology. The authors wish to acknowledge that there are many excellent works in this field that may not be properly discussed here due to the limited space.

8. CONCLUSIONS

Numerical modeling of ultrafast radiative transfer in participating media is indispensable for optical imaging reconstruction and has become a useful alternative to complicated and expensive experiments of many applications in various fields, including biomedicine. Specific biomedical applications of ultrafast laser technology, including cell removal via laser ablation, precision microsurgery, and laser-tissue welding, have been presented along with contributing works in this study. Various numerical methods to accurately determine ultrafast radiative transfer have been presented, and the contributing works for each have been noted. The DOM is one of the more widely used approximate methods for solving the TERT, and has been shown to be accurate when compared with both experimental results and other numerical results. Although it suffers from inherent drawbacks such as numerical diffusion, ray effect, and fixed angular directions, it has the advantage of being computationally efficient and easily implemented; and thus, is one of the more useful tools for numerically determining ultrafast transfer. The FVM offers flexibility in both angular and spatial discretization, making it an important tool for solving the TERT when complex geometries are involved. The FVM still car-

ries the numerical diffusion errors and ray effects. The DA is perhaps the simplest and most efficient tool for determining photon migration in turbid media, but the wide recognition of its limitations and the rapid advances in computing power have greatly impacted its importance. The MCM has been a continually-used method to simulate ultrafast radiative transfer. While drawbacks to the MCM include a lack of computational efficiency and unavoidable statistical errors, its ability to handle almost any physical and geometrical problems and overall flexibility makes it a popular method in the study of ultrafast radiative transfer. However, such a method is hardly useful in the forward modeling for image reconstruction due to its time-consuming nature. Other methods, including the REM, DTM, and IM, have been investigated in more recent years to accompany these four major methods, but have not yet gained popularity. All in all, numerical modeling of ultrafast radiative transfer has had an undeniable impact in many disciplines and will continue to be a driving force in years to come.

Light scattering in biological tissues is highly anisotropic by nature. For ultrafast radiative transfer analysis, the use of isotropic scaling law and reduced scattering coefficient, which is generally acceptable for steady-state radiative transfer, is not appropriate. The prediction with scaled isotropic scattering deviates substantially with the directly anisotropic modeling for signals at early time stages. The ballistic and snake radiation components cannot be predicted accurately with the use of such an approximate technique. To conduct anisotropic scattering modeling, the conservation of both the scattered energy and the asymmetry factor must be observed. For DOM and highly anisotropic scattering media, normalization of the scattering phase function to conserve both conditions must be performed. For FVM, further solid-angle splitting may remedy the situation as well as reduce ray effect, in the sacrifice of substantially increased computer memory usage and CPU time. Normalization of phase function in FVM will reduce the required level of angle splitting and consequently reduce the memory usage and CPU time. When ballistic radiation exists, full normalization of both the ballistic and diffuse radiation components is required.

REFERENCES

- Abergel, R. P., Lyons, R., Dwyer, R., White, R. R., and Uitto, J., Use of lasers for closure of cutaneous wounds: experience with Nd:YAG, argon and CO₂ lasers, *J. Dermatol. Surg. Oncol.*, vol. 12, pp. 1181–1185, 1986.
- Akamatsu, M. and Guo, Z., Ultrafast radiative heat transfer in three-dimensional highly-scattering media subjected to pulse train irradiation, *Numer. Heat Transfer A, Applications*, vol. 59, no. 9, pp. 653–671, 2011.
- Alfano, R. R., Demos, S. G., and Gayen, S. K., Advances in optical imaging of biomedical media, *Ann. NY Acad. Sci.*, vol. 820, pp. 248–270, 1997.
- Alfano, R. R., Demos, S. G., Galland, P., Gaven, S. K., Guo, Y., Ho, P. P., Liang, X., Liu, F., Wang, L., Wang, Q.Z., and Wang, W.B., Time-resolved and nonlinear optical imaging for medical applications, *Ann. N.Y. Acad. Sci.*, vol. 838, pp. 14–28, 1998.

- Anderson, R. R. and Parrish, J. A., Selective photothermolysis: Precise microsurgery by selective absorption of pulsed radiation, *Science*, vol. 220(4596), pp. 524–527, 1983.
- Anghileri, L. J. and Robert, J., *Hyperthermia in Cancer Treatment*, Boca Raton: CRC Press, 1986.
- Arkin, H., Xu, L. X., and Holmes, K. R., Recent developments in modeling heat transfer in blood perfused tissues, *IEEE Trans. Biomed. Eng.*, vol. 41, pp. 97–107, 1994.
- Arridge, S. R., Cope, M., and Delpy, D. T., The theoretical basis for the determination of optical pathlengths in tissue: temporal and frequency analysis, *Phys. Med. Biol.*, vol. 37, no. 7, pp. 1531–1560, 1992.
- Asllanaj, F., Parent, G., and Jeandel, G., Transient radiation and conduction heat transfer in a gray absorbing-emitting medium applied on two-dimensional complex-shaped domains, *Numer. Heat Transfer B, Fundamentals*, vol. 52, no. 2, pp. 179–200, 2007.
- Bass, L. S. and Treat, M. R., Laser tissue welding: a comprehensive review of current and future applications, *Lasers Surg. Med.*, vol. 17, pp. 315–349, 1995.
- Bassani, M., Martelli, F., Zaccanti, G., and Contini, D., Independence of the diffusion coefficient from absorption: experimental and numerical evidence, *Opt. Lett.*, vol. 22, no. 12, pp. 853–855, 1997.
- Benaron, D. A., Hintz, S. R., Villringer, A., Boas, D., Kleinschmidt, A., Frahm, J., Hirth, C., Obrig, H., van Houten, J.C., Kermit, E.L., Cheong, W.F., and Stevenson, D.K., Noninvasive functional imaging of human brain using light, *J. Cereb. Blood Flow Metab.*, vol. 20, pp. 469–477, 2000.
- Boulet, P., Collin, A., and Consalvi, J. P., On the finite volume method and the discrete ordinates method regarding radiative heat transfer in acute forward anisotropic scattering media, *J. Quant. Spectrosc. Radiat. Transfer*, vol. 104, pp. 460–473, 2007.
- Brewster, M. Q. and Yamada, Y., Optical properties of thick, turbid media from picoseconds time-resolved light scattering measurements, *Int. J. Heat Mass Transfer*, vol. 38, no. 14, pp. 2569–2581, 1995.
- Cai, W., Xu, M., Lax, M., and Alfano, R. R., Diffusion coefficient depends on time, not on absorption, *Opt. Lett.*, vol. 27, no. 9, pp. 731–733, 2002.
- Carlson, B. G. and Lathrop, K. D., Transport theory — The method of discrete ordinates, in: H. Greenspan, C. N. Kelber, and D. Okrent (Eds.), *Computing Methods in Reactor Physics*, New York: Gordon & Breach, 1968.
- Chai, J. C., Hsu, P.-f., and Lam, Y. C., Three-dimensional transient radiative transfer modeling using the finite volume method, *J. Quant. Spectrosc. Radiat. Transfer*, vol. 86, pp. 299–313, 2004.
- Chai, J. C., Lee, H. S., and Patankar, S. V., Finite volume method for radiation heat transfer, *J. Thermophys. Heat Transfer*, vol. 8, pp. 419–425, 1994a.
- Chai, J. C., Lee, H. S., and Patankar, S. V., Improved treatment of scattering using the discrete ordinates method, *J. Thermophys. Heat Transfer*, vol. 12, pp. 605–608, 1998.
- Chai, J. C., Lee, H. S., and Patankar, S. V., Ray effect and false scattering in the discrete ordinates method, *Numer. Heat Transfer B, Fundamentals*, vol. 24, pp. 373–389, 1993.
- Chai, J. C., Lee, H. S., and Patankar, S. V., Treatment of irregular geometries using a Cartesian coordinates finite-volume radiation heat transfer procedure, *Numer. Heat Transfer B, Fundamentals*, vol. 26, pp. 225–235, 1994b.
- Chai, J. C., One-dimensional transient radiation heat transfer modeling using a finite-volume method, *Numer. Heat Transfer B, Fundamentals*, vol. 44, no. 2, pp. 187–208, 2003.
- Chai, J. C., Transient radiative transfer in irregular two-dimensional geometries, *J. Quant. Spectrosc. Radiat. Transfer*, vol. 84, pp. 281–294, 2004.

- Chandrasekhar, S., *Radiative Transfer*, New York: Dover Publications, 1960.
- Choi, T. Y. and Grigoropoulos, C. P., Plasma and ablation dynamics in ultrafast laser processing of crystalline silicon, *J. Appl. Phys.*, vol. 92, no. 9, pp. 4918–4925, 2002.
- Chowdhury, I. H., Xu, X., and Weiner, A. M., Ultrafast double-pulse ablation of fused silica, *Appl. Phys. Lett.*, vol. 86, p. 151110, 2005.
- Chui, E. H., Raithby, G. D., and Hughes, P. M. J., Prediction of radiative transfer in cylindrical enclosures with the finite volume method, *J. Thermophys. Heat Transfer*, vol. 6, pp. 605–611, 1992.
- Collin, A., Consalvi, J. L., and Boulet, P., Acute anisotropic scattering in a medium under collimated irradiation, *Int. J. Thermal Sci.*, vol. 50, no. 1, pp. 19–24, 2011.
- Contini, D., Martelli, F., and Zaccanti, G., Photon migration through a turbid slab described by a model based on diffusion approximation. I. Theory, *Appl. Opt.*, vol. 36, no. 19, pp. 4587–4599, 1997.
- Das, C., Trivedi, A., Mitra, K., and Vo-Dinh, T., Experimental and numerical analysis of short-pulse laser interaction with tissue phantoms containing inhomogeneities, *Appl. Opt.*, vol. 42, no. 25, pp. 5173–5180, 2003.
- Durduran, T., Yodh, A. G., Chance, B., and Boas, D. A., Does the photon-diffusion coefficient depend on absorption?, *J. Opt. Soc. Am. A*, vol. 14, no. 12, pp. 3358–3365, 1997.
- Feit, M. D., Rubenchik, A. M., Kim, B.-M., da Silva, L. B., and Perry, M. D., Physical characterization of ultrashort laser pulse drilling of biological tissue, *Appl. Surf. Sci.*, vol. 127, pp. 869–874, 1997.
- Firbank, M., Arridge, S. R., Schweiger, M., and Delpy, D. T., An investigation of light transport through scattering bodies with non-scattering regions, *Phys. Med. Biol.*, vol. 41, pp. 767–783, 1996.
- Fischer, J. P., Dams, J., Gotz, M. H., Kerker, E., Loesel, F. H., Messer, C. J., Niemz, M.H., Suhm, N., and Bille, J.F., Plasma-mediated ablation of brain tissue with picosecond laser pulses, *Appl. Phys. B*, vol. 58, pp. 493–499, 1993.
- Fiveland, W. A., Discrete-ordinates solutions of the radiative transport equation for rectangular enclosures, *J. Heat Transfer*, vol. 106, pp. 699–706, 1984.
- Fiveland, W. A., The selection of discrete ordinate quadrature sets for anisotropic scattering, *Fund. Radiat. Heat Transfer*, ASME HTD, vol. 160, pp. 89–96, 1991.
- Fried, N. M., Hung, V. C., and Walsh, J. T., Jr., Laser tissue welding: Laser spot size and beam profile studies, *IEEE J. Select. Topics Quant. Electron.*, vol. 5, no. 4, pp. 1004–1012, 1999.
- Furutsu, K., Diffusion equation derived from space-time transport equation, *J. Opt. Soc. Am.*, vol. 70, no. 4, pp. 360–366, 1980.
- Furutsu, K. and Yamada, Y., Diffusion approximation for a dissipative random medium and the applications, *Phys. Rev. E*, vol. 50, no. 5, pp. 3634–3640, 1994.
- Gershenson, M., Time-dependent equation for the intensity in the diffusion limit using a higher-order angular expansion, *Phys. Rev. E*, vol. 59, no. 6, pp. 7178–7184, 1999.
- Gu, M. and Sheppard, C. J. R., Three-dimensional image formation in confocal microscopy under ultra-short-laser-pulse illumination, *J. Mod. Opt.*, vol. 42, no. 4, pp. 747–762, 1995.
- Guo, Z. and Kim, K. H., Ultrafast-laser-radiation transfer in heterogeneous tissues with the discrete-ordinates method, *Appl. Opt.*, vol. 42, no. 16, pp. 2897–2905, 2003.
- Guo, Z. and Kumar, S., Discrete-ordinates solution of short-pulsed laser transport in two-dimensional turbid media, *Appl. Opt.*, vol. 40, no. 19, pp. 3156–3163, 2001a.

- Guo, Z. and Kumar, S., Equivalent isotropic scattering formulation for transient short-pulse radiative transfer in anisotropic scattering planar media, *Appl. Opt.*, vol. 39, no. 24, pp. 4411–4417, 2000.
- Guo, Z. and Kumar, S., Radiation element method for transient hyperbolic radiative transfer in plane-parallel inhomogeneous media, *Numer. Heat Transfer B, Fund.*, vol. 39, no. 4, pp. 371–387, 2001b.
- Guo, Z. and Kumar, S., Three-dimensional discrete ordinates-method in transient radiative transfer, *J. Thermophys. Heat Transfer*, vol. 16, no. 3, pp. 289–296, 2002.
- Guo, Z. and Maruyama, S., Scaling anisotropic scattering in radiative transfer in three-dimensional nonhomogeneous media, *Int. Comm. Heat Mass Transfer*, vol. 26, pp. 997–1007, 1999.
- Guo, Z., Aber, J., Garetz, B. A., and Kumar, S., Monte Carlo simulation and experiments of pulsed radiative transfer, *J. Quant. Spectrosc. Radiat. Transfer*, vol. 73, pp. 159–168, 2002.
- Guo, Z., Kumar, S., and Maruyama, S., Transient radiation element method for three-dimensional scattering, absorbing and emitting media, *ASME IMECE 2001, Proc. 2001 ASME IMECE*; New York: ASME, 2001.
- Guo, Z., Kumar, S., and San, K. C., Multidimensional Monte Carlo simulation of short-pulse laser transport in scattering media, *J. Thermophys. Heat Transfer*, vol. 14, no. 4, pp. 504–511, 2000.
- Guo, Z., Wan, S. K., August, D. A., Ying, J., Dunn, S. M., and Semmlow, J. L., Optical imaging of breast tumor through temporal log-slope difference mappings, *Comp. Bio. Med.*, vol. 36, pp. 209–223, 2006.
- Guo, Z., Wan, S. K., Kim, K. H., and Kosaraju, C., Comparing diffusion approximation with radiation transfer analysis for light transport in tissues, *Opt. Rev.*, vol. 10, no. 5, pp. 415–421, 2003.
- Guo, Z., Wang, X. L., and Huan, H., Plasma-mediated ablation of biofilm contamination, *Appl. Surface Sci.*, vol. 257, no. 4, pp. 1247–1253, 2010.
- Hasegawa, Y., Yamada, Y., Tamura, M., and Nomura, Y., Monte Carlo simulation of light transmission through living tissues, *Appl. Opt.*, vol. 30, no. 31, pp. 4515–4520, 1991.
- Hebden, J. C., Veenstra, H., Dehghani, H., Hillman, E. M. C., Schweiger, M., Arridge, S. R., and Delpy, D. T., Three-dimensional time-resolved optical tomography of a conical breast phantom, *Appl. Opt.*, vol. 40, pp. 3278–3287, 2001.
- Henson, J. C., and Malalasekera, W., Comparison of discrete transfer and Monte Carlo methods for radiative heat transfer in three-dimensional non-homogeneous scattering media, *Numer. Heat Transfer A, Applications*, vol. 32, no. 1, pp. 19–36, 1997.
- Hielscher, A. H., Jacques, S. L., Wang, L., and Tittel, F. K., The influence of boundary conditions on the accuracy of diffusion theory in time-resolved reflectance spectroscopy of biological tissues, *Phys. Med. Biol.*, vol. 40, pp. 1957–1975, 1995a.
- Hielscher, A. H., Liu, H., Chance, B., Tittel, F. K., and Jacques, S. L., Phase resolved reflectance spectroscopy on layered turbid media, *Proc. SPIE 1995*, vol. 2389, pp. 248–256, 1995b.
- Hielscher, A. H., Liu, H., Chance, B., Tittel, F. K., and Jacques, S. L., Time-resolved photon emission from layered turbid media, *Appl. Opt.*, vol. 35, no. 4, pp. 719–728, 1996.
- Hong, M. H., Lukyanchuk, B., Huang, S. M., Ong, T. S., Van, L. H., and Chong, T. C., Femtosecond laser application for high capacity optical data storage, *Appl. Phys. A*, vol. 79, pp. 791–794, 2004.
- Howell, J. R., Siegel, R., and Menguc, M. P., *Thermal Radiation Heat Transfer*, 5th ed., New York: CRC Press, 2010.
- Hsu, P.-F. and Lu, X., Temporal reflectance from a light pulse irradiated medium embedded with highly scattering cores, *J. Quant. Spectrosc. Radiat. Transfer*, vol. 107, pp. 429–442, 2007.

- Huang, H. and Guo, Z., Human dermis separation via ultra-short pulsed laser plasma-mediated ablation, *J. Phys. D, Appl.*, vol. 42, 165204, 2009a.
- Huang, H. and Guo, Z., Ultrashort pulsed laser ablation and stripping of freeze-dried dermis, *Lasers Med. Sci.*, vol. 25, pp. 517–524, 2010.
- Huang, H. and Guo, Z., Ultra-short pulsed laser PDMS thin-layer separation and micro-fabrication, *J. Micromech. Microeng.*, vol. 19, 0055007, 2009b.
- Huang, Z. F., Zhou, H. C., and Hsu, P.-F., Improved discrete ordinates method for ray effects mitigation, *J. Heat Transfer*, vol. 103, 044502, 2011.
- Hunter, B. and Guo, Z., Comparison of the discrete-ordinates method and the finite-volume method for steady-state and ultrafast radiative transfer analysis in cylindrical coordinates, *Numer. Heat Transfer B, Fundamentals*, vol. 59, no. 5, pp. 339–359, 2011.
- Hunter, B. and Guo, Z., Conservation of asymmetry factor in phase function discretization for radiative transfer analysis in anisotropic scattering media, *Int. J. Heat Mass Transfer*, vol. 55, pp. 1544–1552, 2012a.
- Hunter, B. and Guo, Z., Phase function normalization for accurate analysis of ultrafast collimated radiative transfer, *Appl. Opt.*, vol. 51, pp. 2192–2201, 2012b.
- Hunter, B. and Guo, Z., Phase-function normalization in the 3D discrete-ordinates solution of radiative transfer — Part I: Conservation of scattered energy and asymmetry factor, *Numer. Heat Transfer B, Fundamentals*, vol. 62, no. 4, pp. 203–222, 2012c.
- Hunter, B. and Guo, Z., Phase-function normalization in the 3D discrete-ordinates solution of radiative transfer — Part II: Benchmark comparisons, *Numer. Heat Transfer B, Fundamentals*, vol. 62, no. 4, pp. 223–242, 2012d.
- Hunter, B. and Guo, Z., Reduction of angle-splitting and computational time for the finite volume method in radiative transfer analysis via phase function normalization, *Int. J. Heat Mass Transfer*, vol. 55, pp. 2449–2460, 2012e.
- Ishimaru, A., Diffusion of light in turbid material, *Appl. Opt.*, vol. 28, no. 12, pp. 2210–2215, 1989.
- Jacques, S. L., Time-resolved propagation of ultrashort laser pulses within turbid tissues, *Appl. Opt.*, vol. 28, no. 12, pp. 2223–2229, 1989.
- Jaunich, M., Raje, S., Kim, K. H., Mitra, K., and Guo, Z., Bio-heat transfer analysis during short pulse laser irradiation of tissues, *Int. J. Heat Mass Transfer*, vol. 51, pp. 5511–5521, 2008.
- Jiao, J. and Guo, Z., Modeling of ultrashort pulsed laser ablation in water and biological tissues in cylindrical coordinates, *Appl. Phys. B*, vol. 103, pp. 195–205, 2011.
- Jiao, J. and Guo, Z., Thermal interaction of short-pulsed laser focused beams with skin tissues, *Phys. Med. Biol.*, vol. 54, pp. 4225–4241, 2009.
- Katika, K. M. and Pilon, L., Ultra-short pulsed laser transport in a multilayered turbid media, *ASME IMECE 2004, Proc. ASME IMECE*, New York: ASME, 2004.
- Kautek, W., Mitterer, S., Kruger, J., Husinsky, W., and Grabner, G., Femtosecond-pulse laser ablation of human corneas, *Appl. Phys. A*, vol. 58, pp. 513–518, 1994.
- Kienle, A. and Patterson, M. S., Improved solutions of the steady-state and the time-resolved diffusion equations for reflectance from a semi-infinite turbid medium, *J. Opt. Soc. Am. A, Opt. Image Sci. Vis.*, vol. 14, no. 1, pp. 246–254, 1997.
- Kienle, A., Glanzmann, T., Wagnieres, G., and van den Bergh, H., Investigation of two-layered turbid media with time-resolved reflectance, *Appl. Opt.*, vol. 37, no. 28, pp. 6852–6862, 1998.

- Kim, B.-M., Feit, M. D., Rubenchik, A. M., Joslin, E. M., Celliers, P. M., Eichler, J., and Da Silva, L.B., Influence of pulse duration on ultrashort laser pulse ablation of biological tissues, *J. Biomed. Opt.*, vol. 6, no. 3, pp. 332–338, 2001.
- Kim, K. H. and Guo, Z., Multi-time-scale heat transfer modeling of turbid tissues exposed to short-pulsed irradiations, *Comput. Meth. Prog. Bio.*, vol. 86, pp. 112–123, 2007.
- Kim, K. H. and Guo, Z., Ultrafast radiation heat transfer in laser tissue welding and soldering, *Numer. Heat Transfer A, Applications*, vol. 46, pp. 23–40, 2004.
- Kim, M. Y., Menon, S., and Baek, S. W., On the transient radiative transfer in a one-dimensional planar medium subjected to radiative equilibrium, *Int. J. Heat Mass Transfer*, vol. 53, pp. 5682–5691, 2010.
- Kim, T. K. and Lee, H., Effect of anisotropic scattering on radiative heat transfer in two-dimensional rectangular enclosures, *Int. J. Heat Mass Transfer*, vol. 31, pp. 1711–1721, 1988.
- Kumar, S. and Mitra, K., Microscale aspects of thermal radiation transport and laser applications, *Adv. Heat Transfer*, vol. 33, pp. 187–294, 1999.
- Lapotko, D. O., Shnip, A. I., Martynenko, O. G., Lukyanova, E. Y., and Klimovich, O. V., Nonstationary heating and phase transitions in a live cell in absorption of laser radiation, *Heat Transfer Research*, vol. 38, no. 8, pp. 695–708, 2007.
- Lathrop, K. D. and Brinkley, F. W., TWOTRAN-II Code, Los Alamos (NM): Los Alamos National Lab., Report No. LA-4848-MS, 1973.
- Lee, H. and Buckius, R. O., Scaling anisotropic scattering in radiation heat transfer for a planar medium, *J. Heat Transfer*, vol. 45, pp. 68–75, 1982.
- Liu, F., Yoo, K. M., and Alfano, R. R., Ultrafast laser-pulse transmission and imaging through biological tissues, *Appl. Opt.*, vol. 32, no. 4, pp. 554–558, 1993.
- Liu, L. H. and Hsu, P.-F., Time shift and superposition method for solving transient radiative transfer equation, *J. Quant. Spectrosc. Radiat. Transfer*, vol. 109, pp. 1297–1308, 2008.
- Liu, L. H., Ruan, L. M., and Tan, H. P., On the discrete ordinates method for radiative heat transfer in anisotropically scattering media, *Int. J. Heat Mass Transfer*, vol. 45, pp. 3259–3262, 2002.
- Liu, X., Du, D., and Mourou, G., Laser ablation and micromachining with ultrashort laser pulses, *IEEE J. Quant. Electron.*, vol. 33, pp. 1706–1716, 1997.
- Loesel, F. H., Fischer, J. P., Gotz, M. H., Horvath, C., Juhasz, T., Noack, F., Suhm, N., and Bille, J.F., Non-thermal ablation of neural tissue with femtosecond laser pulses, *Appl. Phys. B*, vol. 66, pp. 121–128, 1998.
- Lu, X. and Hsu, P.-F., Reverse Monte Carlo for transient radiative transfer in participating media, *J. Heat Transfer*, vol. 126, pp. 621–627, 2004.
- Lu, X. and Hsu, P.-F., Reverse Monte Carlo simulations of light pulse propagation in nonhomogeneous media, *J. Quant. Spectrosc. Radiat. Transfer*, vol. 93, pp. 349–367, 2005.
- Lu, X., Hsu, P.-F., and Chai, J. C., Transient radiative transfer of light pulse propagation in three-dimensional scattering media with finite volume method and integral equation model, *Heat Transfer 2003, Proc. 2003 ASME Summer Heat Transfer Conf.*, 2003 July 21–23; Las Vegas, Nevada, 2003.
- Lubatschowski, H., Heisterkamp, A., Will, F., Serbin, J., Bauer, T., Fallnich, C., Welling, H., Mueller, W., Schwab, B., Singh, A.I., and Ertmer, W., Ultrafast laser pulses for medical applications, *Proc. SPIE 2002*, 4633, doi: 10.1117/12.461386, 2003.
- Maruyama, S. and Aihara, T., Radiation heat transfer between arbitrary three-dimensional absorbing, emitting and scattering media and specular and diffuse surfaces, *ASME J. Heat Transfer*, vol. 119, pp. 129–136, 1997.

- Menguc, M. P. and Viskanta, R., Comparison of radiative transfer approximations for a highly forward scattering planar medium, *J. Quant. Spectrosc. Radiat. Transfer*, vol. 29, pp. 381–394, 1983.
- Mishra, S. C., Chugh, P., Kumar, P., and Mitra, K., Development and comparison of the DTM, the DOM and the FVM formulations for the short-pulse laser transport through a participating medium, *Int. J. Heat Mass Transfer*, vol. 49, pp. 1820–1832, 2006.
- Mitra, K. and Churnside, J. H., Transient radiative transfer equation applied to oceanographic lidar, *Appl. Opt.*, vol. 38, no. 6, pp. 889–895, 1999.
- Mitra, K., and Kumar, S., Development and comparison of models for light-pulse transport through scattering-absorbing media, *Appl. Opt.*, vol. 38, no. 1, pp. 188–196, 1999.
- Mitra, K., Lai, M. S., and Kumar, S., Transient radiation transport in participating media within a rectangular enclosure, *J. Thermophys. Heat Transfer*, vol. 11, no. 3, pp. 409–414, 1997.
- Modest, M. F., *Radiative Heat Transfer*, 2nd ed., New York: Academic Press, 2002.
- Murray, L. W., Su, L., White, G. E., and White, R. A., Cross linking of extracellular matrix proteins: A preliminary report on a possible mechanism of argon laser welding, *Lasers Surg. Med.*, vol. 9, pp. 490–496, 1989.
- Murthy, J. Y. and Mathur, S. R., Finite volume method for radiative heat transfer using unstructured meshes, *J. Thermophys. Heat Transfer*, vol. 12, no. 3, pp. 313–321, 1998.
- Muthukumar, R. and Mishra, S. C., Thermal signatures of a localized inhomogeneity in a 2D participating medium subjected to an ultra-fast step-pulse laser wave, *J. Quant. Spectrosc. Radiat. Transfer*, vol. 109, pp. 705–726, 2008a.
- Muthukumar, R. and Mishra, S. C., Transient response of a planar participating medium subjected to a train of short-pulse radiation, *Int. J. Heat Mass Transfer*, vol. 51, pp. 2418–2432, 2008b.
- Muthukumar, R., Mishra, S. C., Maruyama, S., and Mitra, K., Assessment of signals from a tissue phantom subjected to radiation sources of temporal spans of the order of a nano-, pico-, and femto-second — A numerical study, *Numer. Heat Transfer A, Applications*, vol. 60, no. 2, pp. 154–170, 2011.
- Niemz, M. H., Klancnik, E. G., and Bille, J. F., Plasma-mediated ablation of corneal tissue at 1053 nm using a Nd:YLF oscillator/regenerative amplifier laser, *Lasers Surg. Med.*, vol. 11, pp. 426–431, 1991.
- Ntziachristos, V., Yodh, A. G., Schnall, M., and Chance, B., Concurrent MRI and diffuse optical tomography of breast after indocyanine green enhancement, *Proc. Natl. Acad. Sci.*, vol. 97, pp. 2767–2772, 2000.
- Oraevsky, A. A., Da Silva, L. B., Rubenchik, A. M., Feit, M. D., Glinsky, M. E., Perry, M. D., Mammini, B.M., Small IV, W., and Stuart, B.C., Plasma mediated ablation of biological tissues with nanosecond-to-femtosecond laser pulses: relative role of linear and nonlinear absorption, *IEEE J. Select. Topics Quant. Electron.*, vol. 2, pp. 801–809, 1996.
- Padhi, B. N., Rath, P., Mahapatra, S. K., and Satapathy, A. K., Short pulse collimated radiation with diffusely reflecting boundaries, *Heat Transfer Research*, vol. 42, no. 4, pp. 301–315, 2011.
- Pal, G., Basu, S., Mitra, K., and Vo-Dinh, T., Time-resolved optical tomography using short-pulse laser for tumor detection, *Appl. Opt.*, vol. 45, no. 24, pp. 6270–6282, 2006.
- Patterson, M. S., Chance, B., and Wilson, B. C., Time resolved reflectance and transmittance for the non-invasive measurement of tissue optical properties, *Appl. Opt.*, vol. 28, no. 12, pp. 2331–2336, 1989.
- Quan, H. and Guo, Z., Fast 3D optical imaging with transient fluorescence signals, *Opt. Exp.*, vol. 12, no. 3, pp. 449–457, 2004.

- Rahmani, R. K., Ayasoufi, A., and Molavi, H., Numerical simulation of transient radiative heat transfer applying finite volume method on generalized computational grid, ASME ECTC 2009, *Proc. ASME Early Career Tech. Conf.*, New York: ASME, 2009.
- Raithby, G. D. and Chui, E. H., A finite-volume method for predicting a radiant heat transfer in enclosures with participating media, *J. Heat Transfer*, vol. 112, no. 1, pp. 415–423, 1990.
- Raithby, G. D., Evaluation of discretization errors in finite-volume radiant heat transfer predictions, *Numer. Heat Transfer B, Fundamentals*, vol. 36, pp. 241–264, 1999.
- Rath, P. and Mahapatra, S. K., New formulation of radiative flux in ultrashort time scale with its implications, *J. Thermophys. Heat Transfer*, vol. 26, no. 2, pp. 294–299, 2012.
- Rath, P., Mishra, S. C., Mahanta, P., Saha, U. K., and Mitra, K., Discrete transfer method applied to transient radiative transfer problems in participating medium, *Numer. Heat Transfer A, Applications*, vol. 44, pp. 183–197, 2003.
- Ridouane, E. and Campo, A., Numerical computation of the temperature evolution in the human eye, *Heat Transfer Research*, vol. 37, no. 7, pp. 607–617, 2006.
- Rosseland, S., *Theoretical Astrophysics: Atomic Theory and the Analysis of Stellar Atmospheres and Envelopes*, Oxford: Clarendon Press, 1936.
- Ruan, L. M., Wang, S. G., Qi, H., and Wang, D. L., Analysis of the characteristics of time-resolved signals for transient radiative transfer in scattering participating media, *J. Quant. Spectrosc. Radiat. Transfer*, vol. 111, pp. 2405–2414, 2010.
- Sakami, M., Mitra, K., and Hsu, P.-F., Analysis of light pulse transport through two-dimensional scattering and absorbing media, *J. Quant. Spectrosc. Radiat. Transfer*, vol. 73, pp. 169–173, 2002a.
- Sakami, M., Mitra, K., and Vo-Dinh, T., Analysis of short-pulse laser photon transport through tissues for optical tomography, *Opt. Lett.*, vol. 27, no. 5, pp. 336–338, 2002b.
- Sawetprawichkul, A., Hsu, P.-F., and Mitra, K., Parallel computing of three-dimensional Monte Carlo simulation of transient radiative transfer in participating media, AIAA2002-2901, *Proc. 8th AIAA/ASME Joint Thermophysics & Heat Transfer Conf.*, St. Louis, Missouri, 2002.
- Schmidt, F. E. W., Hebden, J. C., Hillman, E. M. C., Fry, M. E., Schweiger, M., Dehghani, H., Delpy, D.T., and Arridge, S.R., Multiple-slice imaging of a tissue-equivalent phantom by use of time resolved optical tomography, *Appl. Opt.*, vol. 39, pp. 3380–3387, 2000.
- Tan, Z. M. and Hsu, P.-F., Transient radiative transfer in three-dimensional homogeneous and non-homogeneous participating media, *J. Quant. Spectrosc. Radiat. Transfer*, vol. 73, pp. 181–194, 2002.
- Trivedi, A., Basu, S., and Mitra, K., Temporal analysis of reflected optical signals for short pulse laser interaction with nonhomogeneous tissue phantoms, *J. Quant. Spectrosc. Radiat. Transfer*, vol. 93, pp. 337–348, 2005.
- Tromberg, B. J., Shah, N., Lanning, R., Cerussi, A., Expinoza, J., Pham, T., Svaasand, L., and Butler, J., Non-invasive in vivo characterization of breast tumor using photon migration spectroscopy, *Neoplasia*, vol. 2, pp. 1–15, 2000.
- Villringer, A. and Chance, B., Non-invasive optical spectroscopy and imaging of human brain function, *Trends Neurosci.*, vol. 20, pp. 435–42, 1997.
- Wan, S. K., Guo, Z., Kumar, S., Aber, J., and Garetz, B. A., Noninvasive detection of inhomogeneities in turbid media with time-resolved log-slope analysis, *J. Quant. Spectrosc. Radiat. Transfer*, vol. 84, pp. 493–500, 2004.
- Wang, J. M. and Wu, C. Y., Transient radiative transfer in a scattering slab with variable refractive index and diffuse substrate, *Int. J. Heat Mass Transfer*, vol. 53, pp. 3799–3806, 2010.

- Wang, L., Ho, P. P., Liu, C., Zhang, G., and Alfano, R. R., Ballistic 2D imaging through scattering walls using an ultrafast optical kerr gate, *Science*, 253, pp. 769–771, 1991.
- Wang, X. and Guo, Z., Effective removal of adhering cells via ultrashort laser pulses, *Opt. Laser Tech.*, vol. 42, pp. 447–451, 2010.
- Wiscombe, W. J., On initialization, error and flux conservation in the doubling method, *J. Quant. Spectrosc. Radiat. Transfer*, vol. 16, pp. 637–658, 1976.
- Wong, B. T. and Menguc, M. P., Comparison of Monte Carlo techniques to predict the propagation of a collimated beam in participating media, *Numer. Heat Transfer B, Fundamentals*, vol. 42, no. 2, pp. 119–140, 2002.
- Wu, C. Y. and Bhuvanewari, M., Differential approximations for transient radiative transfer in refractive planar media with pulse irradiation, *J. Quant. Spectrosc. Radiat. Transfer*, vol. 110, pp. 389–401, 2009.
- Wu, C. Y. and Wu, S. H., Integral equation formulation for transient radiative transfer in an anisotropically scattering medium, *Int. J. Heat Mass Transfer*, vol. 43, pp. 2009–2020, 2000.
- Wu, C. Y., Monte Carlo simulation of transient radiative transfer in a medium with variable refractive index, *Int. J. Heat Mass Transfer*, vol. 52, pp. 4151–4159, 2009.
- Wu, J., Perelman, L., Dasari, R. R., and Feld, M. S., Fluorescence tomographic imaging in turbid media using early-arriving photons and Laplace transforms, *PNAS*, vol. 94, pp. 8783–8788, 1997.
- Yamada Y., Fundamental studies of photon migration in biological tissues and their application to optical tomography, *Opt. Rev.*, vol. 7, no. 5, pp. 366–374, 2000.
- Yamada, Y. and Hasegawa, Y., Time-dependent FEM analysis of photon migration in biological tissues, *JSME Int. J.*, vol. 39, no. 4, pp. 754–761, 1996.
- Yamada, Y., Light-tissue interaction and optical imaging in biomedicine, *Annu. Rev. Heat Transfer*, vol. 6, pp. 1–59, 1995.
- Yodh, A. and Chance, B., Spectroscopy and imaging with diffuse light, *Phys. Today*, March, pp. 34–40, 1995.
- Yoo, K. M. and Alfano, R. R., Ultrafast time-gated imaging in thick tissues: a step toward optical mammography, *Opt. Lett.*, vol. 18, no. 13, pp. 1092–1094, 1993.
- Yoo, K. M., Liu, F., and Alfano, R. R., When does the diffusion approximation fail to describe photon transport in random media?, *Phys. Rev. Lett.*, vol. 64, pp. 2647–2650, 1990.
- Zaccanti, G., Bruscazioni, P., Ismaelli, A., Carraresi, L., Gurioli, M., and Wei, Q., Transmission of a pulse thin light beam through thick turbid media: experimental results, *J. Opt. Soc. Am.*, vol. 31, pp. 2141–2147, 1992.